DOI:
10.1242/dev.172569

Document Version
Peer reviewed version

First posted online on 29 May 2019 as 10.1242/dev.172569
Access the most recent version at http://dev.biologists.org/lookup/doi/10.1242/dev.172569

Whole organism small molecule screen identifies novel regulators of pancreatic endocrine development

Christian S. M. Helker[1, 2*], Sri-Teja Mullapudi[1], Laura M. Mueller[3], Jens Preussner[4], Sorin Tunaru[5, 6], Oskar Skog[7], Hyouk-Bum Kwon[1], Florian Kreuder[1], Joseph J. Lancman[8, 9], Remy Bonnavion[5], P. Duc Si Dong[8, 9], Mario Looso[4], Stefan Offermanns[5], Ole Korsgren[7], Francesca M. Spagnoli[3] and Didier Y.R. Stainier[1*]

1 Max Planck Institute for Heart and Lung Research, Department of Developmental Genetics, Bad Nauheim, Germany
2 Philipps-University Marburg, Faculty of Biology, Cell Signaling and Dynamics, Marburg, Germany
3 Centre for Stem Cells and Regenerative Medicine, King's College London, United Kingdom
4 Max Planck Institute for Heart and Lung Research, ECCPS Bioinformatics Core Unit, Bad Nauheim, Germany
5 Max Planck Institute for Heart and Lung Research, Department of Pharmacology, Bad Nauheim, Germany
6 Biochemistry Institute of the Romanian Academy, Department of Enzymology, Bucharest, Romania
7 Uppsala University, Department of Immunology, Genetics and Pathology, Uppsala, Sweden
8 Human Genetics Program, Sanford Burnham Prebys Medical Discovery Institute, La Jolla, CA, United States
9 Graduate School of Biomedical Sciences, Sanford Burnham Prebys Medical Discovery Institute, La Jolla, CA, United States

Key words: small molecule screen, Pdx1, β-cells, α-cells, transdifferentiation

*Correspondence to: Christian Helker (Christian.Helker@mpi-bn.mpg.de);
Didier Stainier (Didier.Stainier@mpi-bn.mpg.de)
Department of Developmental Genetics
Max Planck Institute for Heart and Lung Research.
Ludwigstrasse 43, 61231 Bad Nauheim, Germany
Phone: +49 (0) 6032 705-1333
Fax:+49 (0) 6032 705-1304

Abstract

An early step in pancreas development is marked by the expression of the Pdx1 transcription factor within the pancreatic endoderm where it is required for the specification of all endocrine cell types. Subsequently, Pdx1 expression becomes restricted to the β-cell lineage where it plays a central role in β-cell function. This pivotal role of Pdx1 at various stages of pancreas development makes it an attractive target to enhance pancreatic β-cell differentiation and increase β-cell function. In this study, we used a newly generated zebrafish reporter to screen over 8,000 small molecules for modulators of *pdx1* expression. We found four hit compounds and validated their efficacy at different stages of pancreas development. Valproic acid (VPA), a HDAC inhibitor, induces pancreatic endoderm formation, while inhibition of TGF-β signaling leads to the transdifferentiation of α-cells to β-cells. HC Toxin, another HDAC inhibitor, enhances β-cell function in primary mouse and human islets. Thus, using a whole-organism screening strategy, this study identified new *pdx1* expression modulators which can be used to influence different steps in pancreas and β-cell development.

Introduction

Diabetes mellitus is foreseen to be the 7th leading cause of death in 2030 (according to the World Health Organization), warranting an urgent need to identify new therapeutics. During the development of type 2 diabetes, β-cells increase insulin production to compensate for insulin resistance. However, type 2 diabetes only manifests itself once β-cell failure and death occur, resulting in reduced amounts of circulating insulin (Bonner-Weir 2004, 2013).

The transcription factor pancreatic and duodenal homeobox 1 (Pdx1), is a key player in pancreas development and β-cell function/maturation. In vertebrates, Pdx1 is first expressed in the whole pancreatic endoderm, and its importance in early pancreas development has been demonstrated by the global knockout of *Pdx1* which leads to pancreas agenesis and lethality (Jonsson et al. 1994; Offield et al. 1996; Hale et al. 2005). During development, an increase in PDX1 levels in endocrine progenitors is indispensable for their differentiation into β-cells (Bernardo et al. 2008). In addition, forced expression of PDX1 in endocrine progenitors leads to their conversion into β-cells at the expense of α-cells (Yang et al. 2011). In adult mice, PDX1 is specifically expressed in β-cells, and the deletion of *Pdx1* from mature β-cells leads to their dedifferentiation and loss of function (Ahlgren et al. 1998; Gao et al. 2014). In addition, *Pdx1* haploinsufficiency in mice leads to impaired β-cell function and apoptosis (Johnson et al. 2003). In mature β-cells, PDX1 regulates the expression of a whole network of genes important for β-cell function, including *insulin* and *glucokinase* (Ahlgren et al. 1998; Hani et al. 1999; Gao et al. 2014). Notably, and accordingly, MODY4 (Maturity onset of diabetes of the young 4) is caused by mutations in *PDX1* which lead to diabetes due to impaired β-cell function (Fajans et al. 2001). Together, these data point to a central role for PDX1 in pancreas and β-cell development. Therefore, the possibility to regulate the network responsible for β-cell development by modulating a single transcription factor makes PDX1 an interesting target for small molecule screens.

To identify molecular pathways regulating *pdx1* expression, we used the zebrafish, an animal model ideally suited for *in vivo* small molecule screens (Gut et al. 2017); developed novel reporters, and used them to screen 8,256 structurally diverse compounds and subsequently investigated the top hits. Besides known modulators of *pdx1* expression, we identified four interesting compounds which can be used to modulate pancreatic endoderm formation, β-cell specification and/or β-cell function. Notably, VPA treatment increased the formation of the pancreatic endoderm, while inhibition of TGF- β signaling led to the transdifferentiation of α-cells to β-cells. Furthermore, we tested HC Toxin on human islets and in an iPSC-derived pancreatic β-cell differentiation model, and found that it induces β-cell function including enhanced expression of mature β-cell marker genes and enhanced insulin secretion.

Materials and methods

Zebrafish husbandry and strains

All zebrafish husbandry was performed under standard conditions in accordance with institutional (MPG) and national ethical and animal welfare guidelines. Embryos were staged by hours post fertilization (hpf) at 28.5°C (Kimmel et al. 1995). The following lines were used: *Tg(fabp10a:EGFP)*^{as3} (Her, Yeh, and Wu 2003), *Tg(ins:Kaede)*^{jh6} (Pisharath et al. 2007), *Tg(ins:dsRed)*^{m1018} (Shin et al. 2008), *Tg(ins:Hsa.HIST1H2BJ-GFP;ins:DsRed)*^{s960} (Ninov et

al. 2013) abbreviated *Tg(ins:H2B-GFP;ins:DsRed)*, *Tg(pck1:Luciferase)*^{s952} (Gut et al. 2013), *Tg*^{BAC}*(neuroD:EGFP)*^{nl1} (Obholzer et al. 2008), *pdx1*^{sa280} (Kimmel et al. 2015), *insulin*^{bns102} (Mullapudi et al. 2018), *Tg(insulin:loxP:mCherrySTOP:loxP:H2B-GFP; cryaa:Cerulean)*^{s934} (Hesselson et al. 2011), *Tg(sox17:GFP)*^{s870} (Sakaguchi et al. 2006), *Tg(Tp1bglob:H2BmCherry)*^{S939} (Ninov et al. 2012), *Tg(ubb:loxP:CFP:loxP:H2B-mCherry)*^{jh63} (Wang et al. 2015), *Tg*^{BAC}*(arxa:Cre)*^{bns250} (this study), *Tg*^{BAC}*(pdx1:EGFP)*^{bns13} (this study), *Tg*^{BAC}*(pdx1:luciferase2)*^{bns17} (this study) and *Tg(ins:loxP-Eco.NfsB-mCherry-loxP-luciferase)*^{bns152} (this study), abbreviated as *Tg(ins:mCherry)*.

Human islet isolation

Islets were isolated from pancreata procured within the Nordic Network for Clinical Islet Transplantation as previously described (Goto et al. 2004). Consent for organ donation (for clinical transplantation and for use in research) was obtained via an online database (https://www.socialstyrelsen.se/donationsregistret/anmalan) or verbally from the deceased's next of kin by the attending physician. The consent was documented in the medical records of the deceased in accordance with Swedish law and as approved by the Regional Ethics Committee (Dnr 2009/371/2). The experiments using human islets in this study were approved by the Regional Ethics Committee in Uppsala (Dnr 2015/444).

hiPSC culture

Human iPSC lines (iXM001 and BIH004) were maintained on Geltrex-coated (Invitrogen) plates in home-made E8 media, as reported in (Chen et al. 2011) under hypoxic conditions. The medium was changed daily and cells were passaged every ~3 days as cell clumps or single cells using 0.5 mM EDTA (Invitrogen) or Accutase (Invitrogen), respectively. Medium was supplemented with 10 μM Rho-associated protein kinase (ROCK) inhibitor Y-27632 (Sigma) when iPSCs were thawed or passaged as single cells.

Differentiation of pluripotent iPSCs into pancreatic β-like cells

Differentiation was carried out following a 21-day protocol described in Russ et al. (2015). Briefly, iPSCs were dissociated using Accutase and seeded at a density of 5.5 x10^6 cells per well in ultra-low attachment 6-well plates (Thermo Fisher Scientific) in 5.5 ml E8-home medium supplemented with 10 μM ROCK inhibitor, 10 ng/ml Activin A (R&D Systems) and 10 ng/ml Heregulin-b1 (Peprotech). Plates were placed on an orbital shaker at 100 rpm to induce sphere formation at 37°C in a humidified atmosphere containing 5% CO_2.

To induce definitive endoderm differentiation, cell clusters were collected after 36 hrs in a 50-ml falcon tube, washed with PBS and re-suspended in d1 media [RPMI (Invitrogen) containing 0.2% FBS, 1:5.000 ITS (Invitrogen), 100 ng/ml Activin A, and 50 ng/ml WNT3a (R&D Systems)]. Clusters from two wells were combined into one well and distributed into low attachment plates in 5.5 ml d1 media. Subsequently, cell clusters were differentiated into β-like cells by exposure to the appropriate media as previously published (Russ et al. 2015).

Generation of *Tg^{BAC}(pdx1:EGFP)^{bns13}*, *Tg^{BAC}(pdx1:luciferase)^{bns17}*, *TgBAC(arxa:Cre)^{bns250}* and *Tg(ins:loxP-Eco.NfsB-mCherry-loxP-luciferase)^{bns152}* lines

To generate the *pdx1* and *arx* bacterial artificial chromosome (BAC) constructs, we used the BAC clones DKEY-244H6 containing 200 kb of the *pdx1* locus and CH73-369P3 containing 200 kb of the *arx* locus. All recombineering steps were performed as described in (Bussmann et al. 2011) with the modification that we removed the Kanamycin cassette with a flipase for the *arxa^{BAC}:Cre* construct. The following homology arms were used to generate the targeting PCR products of the EGFP_Kan, Luc2_Kan and Cre_Kan cassettes:
pdx1-HA1: 5'-ggcgctggctcatgtgctcgtgtacggcacggtttccccggtctatggca-3'
and *pdx1*-HA2: 5'-aatcgggaagagcattactatccgcctaaccacctgtacaaggactcttg-3';
arxa-HA1: 5'-tgcgagagagagtaacagtcacccactcgagcacgactgaggacgataca-'3
and *arxa*-HA2: 5'-ttgcttttacattcgctccgatcgcggctatcgtcgtcgtactgactgct-'3.
The *Tg^{BAC}(pdx1:EGFP)^{bns13}* and *Tg^{BAC}(pdx1:luciferase)^{bns17}* lines exhibit expression in cell types known to express *pdx1* including β-cells and ductal cells (Ohlsson et al. 1993; Kritzik et al. 1999). We hypothesize that due to the fast transitory stage of the pancreatic endoderm in zebrafish, the *Tg^{BAC}(pdx1:EGFP)^{bns13}* and *Tg^{BAC}(pdx1:luciferase)^{bns17}* lines do not clearly label the pancreatic endoderm. Another explanation would be that the regulatory elements driving *pdx1* expression in the pancreatic endoderm might not be present in the DKEY-244H6. To generate the *Tg(ins:loxP-Eco.NfsB-mCherry-loxP-luciferase)^{bns152}* line, abbreviated as *Tg(ins:mCherry)*, the *loxP Eco.NfsB-mCherry loxP* cassette was amplified by PCR and cloned downstream of the *insulin* promoter together with a 5' *beta-globin* intron. In a second cloning reaction, *luciferase* was amplified by PCR and cloned downstream of *Eco.NfsB-mCherry loxP*. Several founder fish were identified and analyzed. All founder fish exhibited similar patterns of EGFP, Luciferase, Cre, or mCherry expression, ruling out effects related to the site of integration.

Whole Mount in situ Hybridization

Single in situ hybridizations were performed as described (Thisse et al. 2008; Helker et al. 2013).
The following probes were synthesized: *insulin* (Milewski et al. 1998)*; pdx1* was amplified from cDNA of 24 hpf old embryos using the following primers pdx1-forward 5'-caggtagagcagaggtcctga -3' and pdx1-reverse 5'- tcacatcactttaatgtttgtggtaa -3'. The T7 promoter was added to the 5'- end of the reverse primer in a second round of amplification.

Luciferase assay and small molecule screening

Homozygous *Tg^{BAC}(pdx1:luciferase)^{bns17}* animals were outcrossed to AB wild-types to collect large numbers of hemizygous embryos for experiments. At 72 hpf, healthy larvae were selected and washed with egg water before distributing three larvae per well in 200 µl egg water in 96-well plates. Each compound was tested in duplicates. Drugs were used at a concentration of 10 µM in 1% DMSO. After 48 h of treatment, the samples were incubated in Steady Glo (Promega) as described previously (Gut et al. 2013). The bioluminescence signal was analyzed by FLUOstar Omega (BMG LABTECH). Each well was normalized to the average of the DMSO wells in each plate.
An up-regulation of 1.5-fold up in both replicates was assigned as the hit compound threshold. The hits were further tested in validation experiments and by glucose level measurements. The

compounds were not very stable and induction of the *Tg*^{BAC}*(pdx1:luciferase)* reporter at low concentrations was only achieved with freshly ordered compounds. The following chemical libraries were used: LOPAC (Sigma-Aldrich), MicroSource Spectrum Collection, Prestwick Chemical Library, PKIS (Published Kinase Inhibitor Set), Selleckchem Kinase Inhibitory Library, Epigenetic Screening Library, Cayman and TimTec Natural Compound Library. Data analysis was done using a custom script in the statistical language R.

Glucose measurements

After drug treatment, 3 replicates of 5 larvae per condition were homogenized and free glucose levels were determined using a glucose assay kit (BioVision) as described previously (Gut et al. 2013).

qRT-PCR

Total RNA from control and drug-treated MIN6 cells was extracted using a RNeasy Mini Kit (Qiagen). Reverse transcription polymerase chain reaction (RT–PCR) was performed using a SuperScript III First-Strand Synthesis System (Invitrogen) according to manufacturer's instructions. qRT-PCR was carried out to quantify gene expression levels on a CFX connect Real-time System (Bio Rad) with the following Taqman probes: *Pdx1* Mm00435565_m1, *Ins1* Mm01950294_s1. Each sample was normalized to the housekeeping probe *Gapdh* Mm99999915_g1.

Total RNA of β-like cells was isolated using a High Pure RNA Isolation Kit (Roche) or Trizol (Invitrogen). First strand reverse transcription was performed with 1.5 µg RNA using the Transcriptor First Strand cDNA Synthesis Kit (Roche). RT-qPCR was carried out in triplicates using the SYBR Green PCR Master Mix (Thermo Fisher) on a Bio-Rad LightCycler. Results were normalized to *GAPDH* transcripts. Primers used for RT-qPCR are listed in supplementay Table 3. All reactions were performed with annealing at 60°C for 40 cycles. For undetectable transcripts, the cycle number was set to 40 for comparisons.

Confocal Microscopy

Zebrafish larvae were mounted in 1% low melt agarose. Egg water and agarose were supplemented with 19.2 mg/l Tricaine. All fluorescent images were acquired using an upright Zeiss LSM 780, 800 or 880 Confocal microscope. Maximum projection images were analyzed and generated using Imaris (Bitplane).

Immunostaining

Zebrafish larvae were immunostained according to (Lancman et al. 2013). The following primary antibodies were used: Nkx6.1 (DSHB) and Pdx1 (gift from Chris Wright).

Insulin secretion from mouse islets

Pancreatic islets were isolated from 16- to 20-week-old C57BL/6J mice following LiberaseTL (Roche) infusion via the common bile duct to disrupt the pancreatic exocrine tissue and filtration to recover intact islets. Islets were hand-picked and cultured overnight in RPMI1640 supplemented with 10% FBS, 100 units/ml penicillin, and 100 µg/ml streptomycin. Islets were treated with 10 µM of the hit compounds for 12 h in RPMI1640 containing 0.2% BSA, 100 units/ml penicillin, and 100 µg/ml streptomycin. Glucose stimulated insulin secretion was

conducted in KRB buffer containing 4.6 mM KCl, 2.5 mM $CaCl_2$, 1.2 mM $MgSO_4$, 1.2 mM KH_2PO_4, 17.7 mM $NaHCO_3$, 10 mM HEPES, 117 mM NaCl and 0.2% BSA. 10 size-matched islets were pre-incubated for 1 h in KRB containing 3 mM glucose prior to collection of the supernatant from incubations with fresh KRB containing 3 mM and 15 mM glucose. Insulin secretion was assessed with a Mouse Insulin ELISA kit (Alpco) following manufacturer's protocol.

Cell transfection and determination of [Ca2+]

COS-1 cells were seeded in 96-well plates with white walls and transparent bottom and transfected with plasmids containing cDNA encoding a calcium-sensitive bioluminescent fusion protein consisting of aequorin and GFP (Baubet et al. 2000) as well as the indicated receptors using Lipofectamine 2000 (Life Technologies) following manufacturer's instructions. 48 h later, cells were loaded with 5 µM coelenterazine (Promega) in HBSS containing 1.8 mM calcium and 10 mM glucose for 2 h at 37°C. Measurements were performed using a luminometric plate reader (Flexstation 3, Molecular Devices). The area under each calcium transient was calculated using SoftMaxPro software and expressed as area under the curve (AUC).

Glucose-stimulated insulin secretion of human islets

Thirty human islets per well were handpicked under a light microscope into 6-well plates containing 2 ml of CMRL-1066 (ICN Biomedicals, Cosa Mesa, CA) supplemented with 10 mM HEPES, 2 mM L-glutamine, 50 µg/ml Gentamicin, 20 µg/ml Ciprofloxacin, 10 mM nicotinamide, and 10% heat-inactivated human serum. The islets were cultured for 24 h at 37°C with the addition of 10 µM HC Toxin (or DMSO-containing vehicle only) before assessment of glucose-stimulated insulin secretion (GSIS) in a dynamic perifusion system (PERI-4.2, Biorep Technologies, FL, USA). In brief, the islets were transferred to a perifusion chamber and perifused with low (1.6 mM) and high (20 mM) glucose Krebs solution at a flow rate of 100 µl/min at 37°C and collection of the perifusate in 1 min fractions. After a 34 min stabilization period at low glucose, the islets were challenged with high glucose for 15 min and then perifused again with low glucose for 15 min. Insulin was measured in the perifusate fractions with ELISA (Mercodia, Uppsala, Sweden) according to manufacturer's instructions.

Quantifications

β-cell numbers: The average cell number counted in the islets of control DMSO treated larvae was set at 100 percent and the relative changes were calculated. The *pdx1* positive area was quantified by using the area measurement tool from ImageJ.

Statistics

Standard error of the mean and p-values using a 2-tailed t-test were calculated using Microsoft Excel. Statistical significance was indicated with * for $p \leq 0.05$, ** for $p \leq 0.01$, and *** for $p \leq 0.001$.

Results

pdx1 expression dynamics

In order to generate reliable transgenic lines to monitor *pdx1* expression, we chose a BAC (bacterial artificial chromosome) approach over the more commonly used approach of short promoter fragments. This strategy has the clear advantage of having more, or even sometimes all, regulatory elements included in the transgene. We selected a BAC containing 100 kb upstream and 100 kb downstream of *pdx1* and replaced the ATG of *pdx1* with a Luciferase cassette to allow a fast and quantitative readout of *pdx1* expression levels (Fig. S1). An additional BAC transgenic line was made by inserting an EGFP cassette to visualize *pdx1* expression at single cell resolution (Fig. S1). As expected, we observed *pdx1* reporter expression in *insulin* (*ins*) expressing β-cells at 120 hpf (hours post fertilization) (Fig. 1A, B, S1) and coexpression with endogenous Pdx1 (Fig. 1C). To assess the Tg^{BAC}*(pdx1:luciferase2)* (hereafter referred to as Tg^{BAC}*(pdx1*:*Luc2)*) line, we measured *pdx1* promoter activity over the time period of β-cell maturation, i.e., from 48-120 hpf. Coincident with the increase in β-cell maturation, we observed an increase in *pdx1* promoter activity (Fig. 1D). Once β-cell maturation was achieved, *pdx1* promoter activity decreased (Fig. 1D) and free glucose levels dropped (Fig. 1E) (Gut et al. 2013; Mullapudi et al. 2018).

Whole organism screen for modulators of *pdx1* expression

It was recently shown that inhibiting Alk5 (aka Tgfβr1, Transforming growth factor beta receptor 1) in mammalian islets induces the expression of mature β-cell markers, including *Pdx1* (Blum et al. 2014). To test whether the Tg^{BAC}*(pdx1*:*Luc2)* line was indeed functional and responsive to known modulators of *pdx1* expression, we treated 72 hpf Tg^{BAC}*(pdx1:Luc2)* larvae with pharmacological inhibitors of Alk5 for 48 hours followed by a luciferase assay. Indeed, we observed a significant induction of transgene expression (Fig. 2A). Thus, the response of our transgenic reporter to known modulators of *pdx1* expression in mammals supports its use for the identification of novel compounds. The luciferase signal of the Tg^{BAC}*(pdx1:Luc2)* reporter could be modulated by the level of promoter activity, or by the number of β-cells. In order to test this latter hypothesis, we treated 72 hpf Tg^{BAC}*(pdx1:Luc2)* and Tg^{BAC}*(pdx1*:*EGFP)* larvae with a γ-secretase inhibitor (LY411575) to induce secondary islet formation (Parsons et al. 2009; Ninov et al. 2012). Indeed, we observed an increase in the luciferase signal concomitant with the induction of secondary islets (Fig. 2B). To visualize whether secondary islets were also marked by the Tg^{BAC}*(pdx1:EGFP)* reporter, we analyzed the treated animals by confocal microscopy. In DMSO treated control larvae, we did not observe any Tg^{BAC}*(pdx1*:EGFP*)* positive secondary islets. However, in line with the observed increase in luciferase signal, we found EGFP positive cells along the pancreatic duct after treatment with the γ-secretase inhibitor (Fig. 2C).

Next, we designed a high throughput platform to screen for modulators of *pdx1* expression. We decided to use 72 hpf old larvae since metabolic organs are formed by this stage, and these animals are still small enough to be kept in 96 well plates. Three 72 hpf Tg^{BAC}*(pdx1*:*Luc2)* larvae were transferred into each well of 96 well plates and treated in duplicates with small molecule libraries. We decided to use 10 µM, a concentration commonly used in whole organism screens in zebrafish (Andersson et al. 2012; Gut et al. 2013; Tsuji et al. 2014; Gut et al. 2017). After incubating the larvae with the compounds for 48 hours, we performed a visual

inspection of the 96 well plates for signs of toxicity, followed by incubation with a long half-life firefly luciferin to directly measure bioluminescence (Fig. 2D). By screening 8,256 small molecules from diverse chemical libraries, we identified 9 that caused the upregulation of the *pdx1* driven luciferase signal (Fig. 2E, Supplemental Table 1).

Interestingly, among the hit molecules, we found two known regulators of β-cell biology: SKF-86055 and 2',3'-O-Isopropylideneadenosine (Supplemental Table 1). While SKF-86055 inhibits Alk5 and leads to an upregulation of *Pdx1* expression (Blum et al. 2014), 2',3'-O-Isopropylideneadenosine is an adenosine receptor agonist, which increases β-cell replication after β-cell ablation (Andersson et al. 2012). In terms of the other hits, we did not further analyze the PI3K inhibitor due to its known function on the insulin signaling pathway; the MSK1 inhibitor was not commercially available; and the results of the EGFR inhibitor could not be confirmed when using a freshly ordered compound. Dose response curves of the 4 remaining compounds are shown in Fig. S3. Another top hit, Chaulmoogric acid ethyl ester, has not been studied in the context of β-cell biology (Supplemental Table 1). By analyzing the structure of Chaulmoogric acid (Fig. S2), we hypothesized that it could be an agonist for the fatty acid receptor GPR40. Importantly, GPR40 is expressed by β-cells (Itoh et al. 2003), and its agonists have entered clinical trials for the treatment of diabetes (Poitout and Lin 2013). To test this hypothesis, we measured GPR40 activation in COS-1 cells. Following the addition of Chaulmoogric acid, we indeed found a dose-dependent activation of GPR40 (Fig.S4). Overall, the identification of known modulators of β-cell mass and function further validates our screening strategy.

HDAC inhibitors increase pancreatic endoderm at the expense of hepatic endoderm

To analyze whether the hit compounds influence pancreatic endoderm development, we treated wild-type embryos from 5-24 hpf followed by *in situ* hybridization for *pdx1* expression (Fig. 3A). We tested five compounds and found an increase of the *pdx1* positive pancreatic endoderm area in the embryos treated with the HDAC inhibitors Scriptaid and VPA, as well as those treated with the Alk5 inhibitor (Fig. 3B-G). Next, we treated *Tg(sox17:EGFP)* embryos with VPA and analyzed them by confocal microscopy and could indeed confirm the increase in the pancreatic endoderm area (Fig. 3H-J). More strikingly, we found that the area of the hepatic endoderm appeared substantially decreased (Fig. 3H-I).

Alk5 inhibition increases β-cell mass by transdifferentiation of α-cells to β-cells

To analyze whether the hit compounds cause an increase in β-cell mass, we treated *Tg(ins:H2B-GFP;ins:DsRed)* larvae. This strategy allows one to identify newly specified β-cells by the expression of the fast folding fluorophore GFP, while older β-cells will be labeled with GFP as well as with the slow folding fluorophore DsRed (Hesselson et al. 2009). Even though we found no significant increase in β-cell number, there was a trend towards such an increase in larvae treated with the Alk5 inhibitor (Fig. 4A-G). More strikingly, we observed newly specified β-cells (i. e., GFP + DsRed -) after Alk5 inhibition (Fig. 4F 4G, arrowheads). Due to the close developmental relationship between α- and β-cells, we hypothesized that the new β-cells were α-cell derived. To test this hypothesis, we generated *Tg^{BAC}(gcga:Cre)* and *Tg^{BAC}(gcga:CreERT2)* lines to lineage trace α-cells. To our surprise, we found an even more intensive labeling of β-cells in *Tg^{BAC}(gcga:Cre)* and *Tg^{BAC}(gcga:CreERT2)* larvae (data not

shown) than previously reported (Ye et al. 2015). Therefore we decided to generate a *Tg*^{BAC}*(arx:Cre)* line to specifically label α-cells (Fig. S5). We crossed the *Tg*^{BAC}*(arx:Cre)* line to the *Tg(insulin:loxP:mCherrySTOP:loxP:H2B-GFP)* reporter line, in order to specifically label all α-cell derived β-cells by the expression of H2B-GFP (Fig. 4 H-I). By treating the double transgenic larvae with the Alk5 inhibitor, we found a significant increase in α-cell-derived β-cells (Fig.4 H-J). In agreement with these findings, we observed an increase in bihormonal endocrine cells (*Tg(gcg:*EGFP*)*+ and *Tg(ins:*mCherry*)*+) after Alk5 inhibition (Fig.4 K-M).

HDAC inhibitors increase *pdx1* expression and decrease glucose levels

β-cell differentiation can be examined in zebrafish by analyzing the formation of secondary islets following metabolic demand or Notch inhibition (Parsons et al. 2009; Ninov et al. 2013). To analyze whether the increase in *pdx1* promoter driven luciferase activity arises from increased endocrine cell differentiation, we treated the pan-endocrine reporter line *Tg*^{BAC}*(neuroD:EGFP)* with the different HDAC inhibitors. Blocking Notch signaling with the γ-secretase inhibitor DAPT leads to differentiation of endocrine cells along the pancreatic duct (Fig. S6, arrows) (Parsons et al. 2009; Ninov et al. 2012). However, none of the HDAC inhibitors led to an increase in secondary islet formation (Fig. S6, arrows).

Next, we evaluated whether HDAC inhibition could influence β-cell function directly. We speculated that enhanced β-cell function (i. e., insulin secretion) would lead to a change in larval glucose levels. By measuring glucose levels in whole larvae, we found that two out of the three HDAC inhibitors tested could reduce glucose levels (Fig. 5A). These results indicate that HDAC inhibition regulates β-cell function. To further evaluate whether HDAC inhibitors could reduce glucose levels in settings of hyperglycaemia, we treated larvae with the β-adrenergic agonist isoprenaline to induce a strong gluconeogenic response and elevate glucose levels (Fig. 5B) (Gut et al. 2013). Strikingly, the elevated levels of glucose by isoprenaline were completely reversed by co-administration with the HDAC inhibitors HC Toxin, Scriptaid and VPA (Fig. 5B). To analyze whether the HDAC inhibitors reduced glucose levels by inhibiting gluconeogenesis in the liver, we treated *Tg(pck1:luciferase2)* larvae. For all three HDAC inhibitors, we observed a reduction in the luciferase signal (Fig. 5C). To ensure that the glucose level lowering effect was not caused by general toxicity to the animals or their liver, we analyzed the general health of the animals as well as liver morphology and did not observe any obvious phenotypes after treatment with the HDAC inhibitors (Fig. S7).

The glucose lowering effect of HDAC inhibition depends on insulin and Pdx1

To determine whether the glucose level lowering effect of the HDAC inhibitors depended on insulin action, we used *insulin* mutants. Due to the lack of insulin, these mutant larvae exhibit elevated glucose levels. Therefore, any reduction in glucose levels in this model would indicate that the glucose lowering effect is independent of insulin. Among the three HDAC inhibitors analyzed, none of them caused a reduction in glucose levels in the absence of insulin (Fig. 5D), indicating that HC Toxin and Scriptaid enhance β-cell functionality *in vivo* in an insulin dependent manner. To further investigate the most promising compound, HC Toxin, and analyze whether its mechanism of action depended on Pdx1 itself, we used *pdx1* mutants (Kimmel et al. 2015). These mutants are characterized by elevated glucose levels in spite of

the presence of β-cells (Kimmel et al. 2015). We treated *pdx1* mutants with the HDAC inhibitor HC Toxin and strikingly observed reduced glucose levels in heterozygous, but not homozygous mutant animals (Fig. 5E). Together these experiments show that the glucose level lowering effect of HC Toxin depends on Pdx1 and insulin.

HDAC inhibition stimulates the expression of β-cell differentiation markers and the function of mouse and human β-cells

To determine whether the induction of *Pdx1* expression by HDAC inhibition was conserved across species, we used the murine β-cell cell line MIN6, treated the cells with HC Toxin and performed RT-qPCR for *Pdx1* (Fig. 6A) and *Ins1* (Fig. 6B) expression. We found an upregulation of *Pdx1* and *Ins1* expression after treatment with HC Toxin (Fig. 6A, B).

To further investigate the effect of HC Toxin on β-cell differentiation, we turned to a culture system to model human pancreatic β-cell development (Fig. 6C). We used a previously published differentiation protocol (Russ et al. 2015) to efficiently generate insulin-producing cells from human iPSCs, and exposed the cells to HC Toxin during the last step of differentiation. Specifically, iPSCs undergoing differentiation were treated with HC Toxin for 24 h on day 18, and subsequently analyzed by RT-qPCR at day 21 (Fig. 6C, D). Strikingly, we observed an increase in the expression levels of key β-cell transcription factor genes including *PDX1*, *NKX2.2* and *NEUROD1* as well as *INS* after exposure to HC Toxin, suggesting a conserved role for HC Toxin in human β-cell differentiation (Fig. 6D). In addition, the transcript levels of the mature human β-cell transcription factor gene *MAFB* was robustly induced in cells treated with HC Toxin (Fig. 6D). Taken together, these results indicate that HDAC inhibition can efficiently induce the expression of β-cell differentiation markers *in vitro*.

In order to test whether HC Toxin treatment can also modulate the function of primary mammalian β-cells, we tested HC Toxin in a glucose stimulated insulin secretion (GSIS) assay in isolated C57BL/6J mouse islets. We isolated islets from wild-type adult mice and cultured them overnight in the presence of the HDAC inhibitors. On the next day, we performed a GSIS assay and measured released insulin by ELISA. Treatment of islets with HC Toxin was associated with a higher GSIS compared to control islets (Fig. 7A). Given the importance of translating fish and murine model results into a human assay system, we next wanted to test whether the compounds identified in the zebrafish screen would work in human samples. Therefore, an islet perifusion assay was used to assess whether HC Toxin treatment caused an increase in GSIS in freshly isolated human islets. Details about the human donors can be found in Supplemental Table 2. In response to glucose, HC Toxin treated human islets showed significantly increased insulin release compared to DMSO treated controls (Fig. 7B). Thus, consistent with the findings with mouse islets, treatment of human islets with HC Toxin enhanced β-cell function via insulin secretion. These data show that compounds identified in the zebrafish screen can enhance β-cell function in primary human islets.

Discussion

Small molecule screening in animals like zebrafish combines the high-throughput rate of a cellular system with the complex inter-organ physiology of an intact animal (MacRae and Peterson 2015; Gut et al. 2017). Here we describe a novel approach for fast and reliable *in vivo* screening for modulators of *pdx1*expression at the whole organism level. By choosing a 200kb

BAC to generate the reporter we could recapitulate *pdx1* expression in cell types known to express this gene including β-cells and ductal cells (Ohlsson et al. 1993; Kritzik et al. 1999). This observation is in line with the concept that transgenic lines made with BACs recapitulate the endogenous expression more closely compared to those made with short promoter fragments. Besides the validation of our reporter with compounds known to induce *Pdx1* expression in human tissue, we identified compounds with well-known roles in regulating β-cell biology, thus validating the strategy. One example is Chaulmoogric acid which we identified as a novel agonist for the fatty acid receptor GPR40. GPR40 is abundantly expressed by β-cells and it has been shown that the activation of GPR40 by agonists amplifies GSIS (Itoh et al. 2003). In addition, we identified compounds which have not been implicated in the context of pancreas and β-cell development. By using our screening strategy, we identified nine hit molecules which positively modulate the *pdx1* reporter. Among the hit molecules, we identified three structurally diverse HDAC inhibitors: HC Toxin (cyclic peptide HDAC inhibitor), Scriptaid (hydroxamic acid HDAC inhibitor) and VPA (aliphatic acid HDAC inhibitor). Even though several HDAC inhibitors were screened in our assay, only VPA, HC Toxin, Scriptaid and TSA (data not shown) could reproducibly induce the *pdx1* reporter. In addition, the two benzamide HDAC inhibitors, MS-275 and CI-994, induced the *pdx1* reporter, but only at 50 µM (data not shown).

TSA and VPA have recently been shown to enhance the pool of the proendocrine lineage (Haumaitre et al. 2009). This observation is in line with our results showing that VPA increases pancreatic endoderm size which subsequently leads to an increase in the proendocrine lineage. In addition, work from Noel et al. (2008) showed a reduced liver size in *hdac1* mutants, which is in line with our observations showing that VPA treatment decreased the area of the hepatic endoderm. It will be interesting to analyze the pancreatic endoderm in the *hdac1* mutants. In zebrafish, VPA treatment has been shown to disrupt the clustering of endocrine cells (Li et al. 2016). However, this disruption could be caused by the early and long treatment period used which included gastrulation (5 to 72 hpf). HC Toxin and Scriptaid have recently been shown to enhance glucose uptake and metabolism in mouse skeletal muscle (Tan et al. 2015; Gaur et al. 2017). However, these studies only focused on mechanisms downstream of insulin. It has also been shown that HDAC inhibition protects β-cells from cytokine induced apoptosis (Larsen et al. 2007). Since *Pdx1* haploinsufficiency also leads to β-cell apoptosis (Johnson et al. 2003), it would be interesting to test whether increase of *Pdx1* expression by HDAC inhibition protects β-cells from cytokine induced apoptosis. In addition to these published observations, our data clearly show that Scriptaid and HC Toxin regulate glucose homeostasis by modulating β-cell function. The reduction in whole body glucose levels could be due to an increase in insulin secretion by β-cells, increased glucose uptake by target tissues such as muscle and reduced gluconeogenesis in the liver. Even though VPA caused only a mild effect in our assays compared to Scriptaid and HC Toxin, data obtained from human patients treated with VPA show increased postprandial insulin levels (Luef et al. 2002), confirming our observations.

HDACs alter chromatin structure and transcriptional activity by removing lysine acetylation on histones (Seto et al. 2014). However, several non-histone proteins are also regulated by lysine acetylation (Seto et al. 2014). Therefore, it is not clear whether the mechanism of action of VPA, HC Toxin and Scriptaid is based on epigenetic regulation by chromatin or on posttranslational modifications of non-chromatin proteins. In the oncology field, it has been

shown that HDAC inhibitors have anti-proliferative effects on cancer cells, and several of them are now used in clinical trials (West et al. 2014). However, a clear mechanism of action has not yet been attained. Recently, it has been shown that protein acetylation can alter the metabolism of the cell (Zhao et al. 2010), which can be achieved by post-translational modification of non-histone cytoplasmic and mitochondrial proteins (Anderson et al. 2012; Kim et al. 2006). In fact, several HDACs have been localized in the cytoplasm and mitochondria (Bakin et al. 2004; Drazic et al. 2016; Herr et al. 2018). On a functional level, it has been shown that treatment with HDAC inhibitors causes a rapid increase in mitochondrial activity, arguing against a regulation at the level of the chromatin (Becker et al. 2018). The observation of an increase in GSIS as early as five hours after treatment (data not shown) indicates that this response is independent of epigenetic regulation or cell proliferation. Recent work has been reported that the deletion of HDAC3 in β-cells led to glucose intolerance (Chen et al. 2016). However, simultaneously, another group reported that the deletion of HDAC3 in β-cells improved glucose tolerance (Remsberg et al. 2017). Of interest, Remsberg et al. (2017) also showed that a PDX1 motif is enriched under HDAC3 binding peaks. Together with our work, these finding lead us to speculate that HDACs regulate *Pdx1* expression to modulate β-cell function.

A new hope for the treatment of type 1 diabetes is the transplantation of stem cell derived β-cells. Recently, several groups have reported the differentiation of β-like-cells from stem cells (Pagliuca et al. 2014; Rezania et al. 2014; Russ et al. 2015). However, the efficiency in generating β-like-cells is still low and varies between groups. So far, HDAC inhibitors have not been used in β–cell differentiation protocols. Our findings indicate that the addition of HC Toxin can efficiently induce the expression of differentiation markers *in vitro*, not only illustrating the value of our screen, but also adding another modulator to further optimize protocols for β-like-cell generation *in vitro*. Notably, the Alk5 inhibitor which we identified in our zebrafish screen, has been shown to upregulate *Pdx1* expression in human islets (Blum et al. 2014), and it is already in use in β-cell differentiation protocols (Pagliuca et al. 2014; Rezania et al. 2014; Russ et al. 2015).

Recent work has highlighted the potential of α-cells as a source for new β-cells during regeneration (Thorel et al. 2010; Courtney et al. 2013). Follow up studies reported GABA as a possible signal driving α to β-cell transdifferentiation (Ben-Othman et al. 2017; Li et al. 2017). However, independent studies have now shown that the use of the *Gcg* promoter for lineage tracing might have led to a misinterpretation of the results (van der Meulen et al. 2018; Ackermann et al. 2018). In agreement with this concern, we observed intensive β-cell labeling with our newly generated Tg^{BAC}*(gcga:Cre)* and Tg^{BAC}*(gcga:CreERT2)* lines (data not shown), which might be caused by the expression of *gcga* by β-cells (Tarifeno-Saldivia et al. 2017). Since it has been shown that *arxa* is specifically expressed in mature α but not β-cells (Tarifeno-Saldivia et al. 2017), we decided to generate a Tg^{BAC}*(arxa:Cre)* line to specifically label α-cells. Our results highlight a novel role for TGF-β signaling during α to β-cell transdifferentiation. The potential role of TGF-β signaling in α-cells is in line with recent work profiling different endocrine cell types and showing the specific expression of the *TGF-β receptor 2* gene in α-cells (Tarifeno-Saldivia et al. 2017). Further work is needed to elucidate how TGF-β signaling negatively regulates α to β-cell transdifferentiation.

References

Ackermann, A. M., N. G. Moss, and K. H. Kaestner. 2018. 'GABA and Artesunate Do Not Induce Pancreatic alpha-to-beta Cell Transdifferentiation In Vivo', *Cell Metab*.

Ahlgren, U., J. Jonsson, L. Jonsson, K. Simu, and H. Edlund. 1998. 'beta-cell-specific inactivation of the mouse Ipf1/Pdx1 gene results in loss of the beta-cell phenotype and maturity onset diabetes', *Genes Dev*, 12: 1763-8.

Anderson, K. A., and M. D. Hirschey. 2012. 'Mitochondrial protein acetylation regulates metabolism', *Essays Biochem*, 52: 23-35.

Andersson, O., B. A. Adams, D. Yoo, G. C. Ellis, P. Gut, R. M. Anderson, M. S. German, and D. Y. Stainier. 2012. 'Adenosine signaling promotes regeneration of pancreatic beta cells in vivo', *Cell Metab*, 15: 885-94.

Bakin, R. E., and M. O. Jung. 2004. 'Cytoplasmic sequestration of HDAC7 from mitochondrial and nuclear compartments upon initiation of apoptosis', *J Biol Chem*, 279: 51218-25.

Baubet, V., H. Le Mouellic, A. K. Campbell, E. Lucas-Meunier, P. Fossier, and P. Brulet. 2000. 'Chimeric green fluorescent protein-aequorin as bioluminescent Ca2+ reporters at the single-cell level', *Proc Natl Acad Sci U S A*, 97: 7260-5.

Becker, L., M. S. Nogueira, C. Klima, M. H. de Angelis, and S. Peleg. 2018. 'Rapid and transient oxygen consumption increase following acute HDAC/KDAC inhibition in Drosophila tissue', *Sci Rep*, 8: 4199.

Ben-Othman, N., A. Vieira, M. Courtney, F. Record, E. Gjernes, F. Avolio, B. Hadzic, N. Druelle, T. Napolitano, S. Navarro-Sanz, S. Silvano, K. Al-Hasani, A. Pfeifer, S. Lacas-Gervais, G. Leuckx, L. Marroqui, J. Thevenet, O. D. Madsen, D. L. Eizirik, H. Heimberg, J. Kerr-Conte, F. Pattou, A. Mansouri, and P. Collombat. 2017. 'Long-Term GABA Administration Induces Alpha Cell-Mediated Beta-like Cell Neogenesis', *Cell*, 168: 73-85 e11.

Bernardo, A. S., C. W. Hay, and K. Docherty. 2008. 'Pancreatic transcription factors and their role in the birth, life and survival of the pancreatic beta cell', *Mol Cell Endocrinol*, 294: 1-9.

Blum, B., A. N. Roose, O. Barrandon, R. Maehr, A. C. Arvanites, L. S. Davidow, J. C. Davis, Q. P. Peterson, L. L. Rubin, and D. A. Melton. 2014. 'Reversal of beta cell de-differentiation by a small molecule inhibitor of the TGFbeta pathway', *Elife*, 3: e02809.

Bussmann, J., and S. Schulte-Merker. 2011. 'Rapid BAC selection for tol2-mediated transgenesis in zebrafish', *Development*, 138: 4327-32.

Chen, G., D. R. Gulbranson, Z. Hou, J. M. Bolin, V. Ruotti, M. D. Probasco, K. Smuga-Otto, S. E. Howden, N. R. Diol, N. E. Propson, R. Wagner, G. O. Lee, J. Antosiewicz-Bourget, J. M. Teng, and J. A. Thomson. 2011. 'Chemically defined conditions for human iPSC derivation and culture', *Nat Methods*, 8: 424-9.

Chen, W. B., L. Gao, J. Wang, Y. G. Wang, Z. Dong, J. Zhao, Q. S. Mi, and L. Zhou. 2016. 'Conditional ablation of HDAC3 in islet beta cells results in glucose intolerance and enhanced susceptibility to STZ-induced diabetes', *Oncotarget*, 7: 57485-97.

Courtney, M., E. Gjernes, N. Druelle, C. Ravaud, A. Vieira, N. Ben-Othman, A. Pfeifer, F. Avolio, G. Leuckx, S. Lacas-Gervais, F. Burel-Vandenbos, D. Ambrosetti, J. Hecksher-Sorensen, P. Ravassard, H. Heimberg, A. Mansouri, and P. Collombat. 2013. 'The inactivation of Arx in pancreatic alpha-cells triggers their neogenesis and conversion into functional beta-like cells', *PLoS Genet*, 9: e1003934.

Drazic, A., L. M. Myklebust, R. Ree, and T. Arnesen. 2016. 'The world of protein acetylation', *Biochim Biophys Acta*, 1864: 1372-401.

Fajans, S. S., G. I. Bell, and K. S. Polonsky. 2001. 'Molecular mechanisms and clinical pathophysiology of maturity-onset diabetes of the young', *N Engl J Med*, 345: 971-80.

Gao, T., B. McKenna, C. Li, M. Reichert, J. Nguyen, T. Singh, C. Yang, A. Pannikar, N. Doliba, T. Zhang, D. A. Stoffers, H. Edlund, F. Matschinsky, R. Stein, and B. Z. Stanger. 2014. 'Pdx1 maintains beta cell identity and function by repressing an alpha cell program', *Cell Metab*, 19: 259-71.

Gaur, V., T. Connor, K. Venardos, D. C. Henstridge, S. D. Martin, C. Swinton, S. Morrison, K. Aston-Mourney, S. M. Gehrig, R. van Ewijk, G. S. Lynch, M. A. Febbraio, G. R. Steinberg, M. Hargreaves, K. R. Walder, and S. L. McGee. 2017. 'Scriptaid enhances skeletal muscle insulin action and cardiac function in obese mice', *Diabetes Obes Metab*, 19: 936-43.

Goto, M., T. M. Eich, M. Felldin, A. Foss, R. Kallen, K. Salmela, A. Tibell, G. Tufveson, K. Fujimori, M. Engkvist, and O. Korsgren. 2004. 'Refinement of the automated method for human islet isolation and presentation of a closed system for in vitro islet culture', *Transplantation*, 78: 1367-75.

Gut, P., B. Baeza-Raja, O. Andersson, L. Hasenkamp, J. Hsiao, D. Hesselson, K. Akassoglou, E. Verdin, M. D. Hirschey, and D. Y. Stainier. 2013. 'Whole-organism screening for gluconeogenesis identifies activators of fasting metabolism', *Nat Chem Biol*, 9: 97-104.

Gut, P., S. Reischauer, D. Y. R. Stainier, and R. Arnaout. 2017. 'Little Fish, Big Data: Zebrafish as a Model for Cardiovascular and Metabolic Disease', *Physiol Rev*, 97: 889-938.

Hale, M. A., H. Kagami, L. Shi, A. M. Holland, H. P. Elsasser, R. E. Hammer, and R. J. MacDonald. 2005. 'The homeodomain protein PDX1 is required at mid-pancreatic development for the formation of the exocrine pancreas', *Dev Biol*, 286: 225-37.

Hani, E. H., D. A. Stoffers, J. C. Chevre, E. Durand, V. Stanojevic, C. Dina, J. F. Habener, and P. Froguel. 1999. 'Defective mutations in the insulin promoter factor-1 (IPF-1) gene in late-onset type 2 diabetes mellitus', *J Clin Invest*, 104: R41-8.

Haumaitre, C., O. Lenoir, and R. Scharfmann. 2009. 'Directing cell differentiation with small-molecule histone deacetylase inhibitors: the example of promoting pancreatic endocrine cells', *Cell Cycle*, 8: 536-44.

Helker, C. S., A. Schuermann, T. Karpanen, D. Zeuschner, H. G. Belting, M. Affolter, S. Schulte-Merker, and W. Herzog. 2013. 'The zebrafish common cardinal veins develop by a novel mechanism: lumen ensheathment', *Development*, 140: 2776-86.

Her, G. M., Y. H. Yeh, and J. L. Wu. 2003. '435-bp liver regulatory sequence in the liver fatty acid binding protein (L-FABP) gene is sufficient to modulate liver regional expression in transgenic zebrafish', *Dev Dyn*, 227: 347-56.

Herr, D. J., M. Baarine, S. E. Aune, X. Li, L. E. Ball, J. J. Lemasters, C. C. Beeson, J. C. Chou, and D. R. Menick. 2018. 'HDAC1 localizes to the mitochondria of cardiac myocytes and contributes to early cardiac reperfusion injury', *J Mol Cell Cardiol*, 114: 309-19.

Hesselson, D., R. M. Anderson, M. Beinat, and D. Y. Stainier. 2009. 'Distinct populations of quiescent and proliferative pancreatic beta-cells identified by HOTcre mediated labeling', *Proc Natl Acad Sci U S A*, 106: 14896-901.

Hesselson, D., R. M. Anderson, and D. Y. Stainier. 2011. 'Suppression of Ptf1a activity induces acinar-to-endocrine conversion', *Curr Biol*, 21: 712-7.

Itoh, Y., Y. Kawamata, M. Harada, M. Kobayashi, R. Fujii, S. Fukusumi, K. Ogi, M. Hosoya, Y. Tanaka, H. Uejima, H. Tanaka, M. Maruyama, R. Satoh, S. Okubo, H. Kizawa, H. Komatsu, F. Matsumura, Y. Noguchi, T. Shinohara, S. Hinuma, Y. Fujisawa, and M. Fujino. 2003. 'Free fatty acids regulate insulin secretion from pancreatic beta cells through GPR40', *Nature*, 422: 173-6.

Johnson, J. D., N. T. Ahmed, D. S. Luciani, Z. Han, H. Tran, J. Fujita, S. Misler, H. Edlund, and K. S. Polonsky. 2003. 'Increased islet apoptosis in Pdx1+/- mice', *J Clin Invest*, 111: 1147-60.

Jonsson, J., L. Carlsson, T. Edlund, and H. Edlund. 1994. 'Insulin-promoter-factor 1 is required for pancreas development in mice', *Nature*, 371: 606-9.

Kim, S. C., R. Sprung, Y. Chen, Y. Xu, H. Ball, J. Pei, T. Cheng, Y. Kho, H. Xiao, L. Xiao, N. V. Grishin, M. White, X. J. Yang, and Y. Zhao. 2006. 'Substrate and functional diversity of lysine acetylation revealed by a proteomics survey', *Mol Cell*, 23: 607-18.

Kimmel, C. B., W. W. Ballard, S. R. Kimmel, B. Ullmann, and T. F. Schilling. 1995. 'Stages of embryonic development of the zebrafish', *Dev Dyn*, 203: 253-310.

Kimmel, R. A., S. Dobler, N. Schmitner, T. Walsen, J. Freudenblum, and D. Meyer. 2015. 'Diabetic pdx1-mutant zebrafish show conserved responses to nutrient overload and anti-glycemic treatment', *Sci Rep*, 5: 14241.

Kritzik, M. R., E. Jones, Z. Chen, M. Krakowski, T. Krahl, A. Good, C. Wright, H. Fox, and N. Sarvetnick. 1999. 'PDX-1 and Msx-2 expression in the regenerating and developing pancreas', *J Endocrinol*, 163: 523-30.

Lancman, J. J., N. Zvenigorodsky, K. P. Gates, D. Zhang, K. Solomon, R. K. Humphrey, T. Kuo, L. Setiawan, H. Verkade, Y. I. Chi, U. S. Jhala, C. V. Wright, D. Y. Stainier, and P. D. Dong. 2013. 'Specification of hepatopancreas progenitors in zebrafish by hnf1ba and wnt2bb', *Development*, 140: 2669-79.

Larsen, L., M. Tonnesen, S. G. Ronn, J. Storling, S. Jorgensen, P. Mascagni, C. A. Dinarello, N. Billestrup, and T. Mandrup-Poulsen. 2007. 'Inhibition of histone deacetylases prevents cytokine-induced toxicity in beta cells', *Diabetologia*, 50: 779-89.

Li, J., T. Casteels, T. Frogne, C. Ingvorsen, C. Honore, M. Courtney, K. V. M. Huber, N. Schmitner, R. A. Kimmel, R. A. Romanov, C. Sturtzel, C. H. Lardeau, J. Klughammer, M. Farlik, S. Sdelci, A. Vieira, F. Avolio, F. Briand, I. Baburin, P. Majek, F. M. Pauler, T. Penz, A. Stukalov, M. Gridling, K. Parapatics, C. Barbieux, E. Berishvili, A. Spittler, J. Colinge, K. L. Bennett, S. Hering, T. Sulpice, C. Bock, M. Distel, T. Harkany, D. Meyer, G. Superti-Furga, P. Collombat, J. Hecksher-Sorensen, and S. Kubicek. 2017. 'Artemisinins Target GABAA Receptor Signaling and Impair alpha Cell Identity', *Cell*, 168: 86-100 e15.

Li, L., F. Bonneton, M. Tohme, L. Bernard, X. Y. Chen, and V. Laudet. 2016. 'In Vivo Screening Using Transgenic Zebrafish Embryos Reveals New Effects of HDAC Inhibitors Trichostatin A and Valproic Acid on Organogenesis', *PLoS One*, 11: e0149497.

Luef, G., I. Abraham, E. Trinka, A. Alge, J. Windisch, G. Daxenbichler, I. Unterberger, K. Seppi, M. Lechleitner, G. Kramer, and G. Bauer. 2002. 'Hyperandrogenism, postprandial hyperinsulinism and the risk of PCOS in a cross sectional study of women with epilepsy treated with valproate', *Epilepsy Res*, 48: 91-102.

MacRae, C. A., and R. T. Peterson. 2015. 'Zebrafish as tools for drug discovery', *Nat Rev Drug Discov*, 14: 721-31.

Milewski, W. M., S. J. Duguay, S. J. Chan, and D. F. Steiner. 1998. 'Conservation of PDX-1 structure, function, and expression in zebrafish', *Endocrinology*, 139: 1440-9.

Mullapudi, S. T., C. S. Helker, G. L. Boezio, H. M. Maischein, A. M. Sokol, S. Guenther, H. Matsuda, S. Kubicek, J. Graumann, Y. H. C. Yang, and D. Y. Stainier. 2018. 'Screening for insulin-independent pathways that modulate glucose homeostasis identifies androgen receptor antagonists', *Elife*, 7.

Ninov, N., M. Borius, and D. Y. Stainier. 2012. 'Different levels of Notch signaling regulate quiescence, renewal and differentiation in pancreatic endocrine progenitors', *Development*, 139: 1557-67.

Ninov, N., D. Hesselson, P. Gut, A. Zhou, K. Fidelin, and D. Y. Stainier. 2013. 'Metabolic regulation of cellular plasticity in the pancreas', *Curr Biol*, 23: 1242-50.

Obholzer, N., S. Wolfson, J. G. Trapani, W. Mo, A. Nechiporuk, E. Busch-Nentwich, C. Seiler, S. Sidi, C. Sollner, R. N. Duncan, A. Boehland, and T. Nicolson. 2008. 'Vesicular glutamate transporter 3 is required for synaptic transmission in zebrafish hair cells', *J Neurosci*, 28: 2110-8.

Offield, M. F., T. L. Jetton, P. A. Labosky, M. Ray, R. W. Stein, M. A. Magnuson, B. L. Hogan, and C. V. Wright. 1996. 'PDX-1 is required for pancreatic outgrowth and differentiation of the rostral duodenum', *Development*, 122: 983-95.

Ohlsson, H., K. Karlsson, and T. Edlund. 1993. 'IPF1, a homeodomain-containing transactivator of the insulin gene', *EMBO J*, 12: 4251-9.

Pagliuca, F. W., J. R. Millman, M. Gurtler, M. Segel, A. Van Dervort, J. H. Ryu, Q. P. Peterson, D. Greiner, and D. A. Melton. 2014. 'Generation of functional human pancreatic beta cells in vitro', *Cell*, 159: 428-39.

Parsons, M. J., H. Pisharath, S. Yusuff, J. C. Moore, A. F. Siekmann, N. Lawson, and S. D. Leach. 2009. 'Notch-responsive cells initiate the secondary transition in larval zebrafish pancreas', *Mech Dev*, 126: 898-912.

Pisharath, H., J. M. Rhee, M. A. Swanson, S. D. Leach, and M. J. Parsons. 2007. 'Targeted ablation of beta cells in the embryonic zebrafish pancreas using E. coli nitroreductase', *Mech Dev*, 124: 218-29.

Poitout, V., and D. C. Lin. 2013. 'Modulating GPR40: therapeutic promise and potential in diabetes', *Drug Discov Today*, 18: 1301-8.

Remsberg, J. R., B. N. Ediger, W. Y. Ho, M. Damle, Z. Li, C. Teng, C. Lanzillotta, D. A. Stoffers, and M. A. Lazar. 2017. 'Deletion of histone deacetylase 3 in adult beta cells improves glucose tolerance via increased insulin secretion', *Mol Metab*, 6: 30-37.

Rezania, A., J. E. Bruin, P. Arora, A. Rubin, I. Batushansky, A. Asadi, S. O'Dwyer, N. Quiskamp, M. Mojibian, T. Albrecht, Y. H. Yang, J. D. Johnson, and T. J. Kieffer. 2014. 'Reversal of diabetes with insulin-producing cells derived in vitro from human pluripotent stem cells', *Nat Biotechnol*, 32: 1121-33.

Russ, H. A., A. V. Parent, J. J. Ringler, T. G. Hennings, G. G. Nair, M. Shveygert, T. Guo, S. Puri, L. Haataja, V. Cirulli, R. Blelloch, G. L. Szot, P. Arvan, and M. Hebrok. 2015. 'Controlled induction of human pancreatic progenitors produces functional beta-like cells in vitro', *EMBO J*, 34: 1759-72.

Sakaguchi, T., Y. Kikuchi, A. Kuroiwa, H. Takeda, and D. Y. Stainier. 2006. 'The yolk syncytial layer regulates myocardial migration by influencing extracellular matrix assembly in zebrafish', *Development*, 133: 4063-72.

Seto, E., and M. Yoshida. 2014. 'Erasers of histone acetylation: the histone deacetylase enzymes', *Cold Spring Harb Perspect Biol*, 6: a018713.

Shin, C. H., W. S. Chung, S. K. Hong, E. A. Ober, H. Verkade, H. A. Field, J. Huisken, and D. Y. Stainier. 2008. 'Multiple roles for Med12 in vertebrate endoderm development', *Dev Biol*, 317: 467-79.

Tan, H. W., A. Y. Sim, S. L. Huang, Y. Leng, and Y. C. Long. 2015. 'HC toxin (a HDAC inhibitor) enhances IRS1-Akt signalling and metabolism in mouse myotubes', *J Mol Endocrinol*, 55: 197-207.

Tarifeno-Saldivia, E., A. Lavergne, A. Bernard, K. Padamata, D. Bergemann, M. L. Voz, I. Manfroid, and B. Peers. 2017. 'Transcriptome analysis of pancreatic cells across distant species highlights novel important regulator genes', *BMC Biol*, 15: 21.

Thisse, C., and B. Thisse. 2008. 'High-resolution in situ hybridization to whole-mount zebrafish embryos', *Nat Protoc*, 3: 59-69.

Thorel, F., V. Nepote, I. Avril, K. Kohno, R. Desgraz, S. Chera, and P. L. Herrera. 2010. 'Conversion of adult pancreatic alpha-cells to beta-cells after extreme beta-cell loss', *Nature*, 464: 1149-54.

Tsuji, N., N. Ninov, M. Delawary, S. Osman, A. S. Roh, P. Gut, and D. Y. Stainier. 2014. 'Whole organism high content screening identifies stimulators of pancreatic beta-cell proliferation', *PLoS One*, 9: e104112.

van der Meulen, T., S. Lee, E. Noordeloos, C. J. Donaldson, M. W. Adams, G. M. Noguchi, A. M. Mawla, and M. O. Huising. 2018. 'Artemether Does Not Turn alpha Cells into beta Cells', *Cell Metab*, 27: 218-25 e4.

Wang, Y. J., J. T. Park, M. J. Parsons, and S. D. Leach. 2015. 'Fate mapping of ptf1a-expressing cells during pancreatic organogenesis and regeneration in zebrafish', *Dev Dyn*, 244: 724-35.

Weir, G. C., and S. Bonner-Weir. 2004. 'Five stages of evolving beta-cell dysfunction during progression to diabetes', *Diabetes*, 53 Suppl 3: S16-21.

Weir, G. C., and S. Bonner-Weir. 2013. 'Islet beta cell mass in diabetes and how it relates to function, birth, and death', *Ann N Y Acad Sci*, 1281: 92-105.

West, A. C., and R. W. Johnstone. 2014. 'New and emerging HDAC inhibitors for cancer treatment', *J Clin Invest*, 124: 30-9.

Yang, Y. P., F. Thorel, D. F. Boyer, P. L. Herrera, and C. V. Wright. 2011. 'Context-specific alpha- to-beta-cell reprogramming by forced Pdx1 expression', *Genes Dev*, 25: 1680-5.

Ye, L., M. A. Robertson, D. Hesselson, D. Y. Stainier, and R. M. Anderson. 2015. 'Glucagon is essential for alpha cell transdifferentiation and beta cell neogenesis', *Development*, 142: 1407-17.

Zhao, S., W. Xu, W. Jiang, W. Yu, Y. Lin, T. Zhang, J. Yao, L. Zhou, Y. Zeng, H. Li, Y. Li, J. Shi, W. An, S. M. Hancock, F. He, L. Qin, J. Chin, P. Yang, X. Chen, Q. Lei, Y. Xiong, and K. L. Guan. 2010. 'Regulation of cellular metabolism by protein lysine acetylation', *Science*, 327: 1000-4.

Acknowledgements

We thank Dirk Meyer and Robin Kimmel for kindly providing the *pdx1*^{sa280} fish line, Sonja Sievers for advice regarding the chemical libraries, Marianne Ploch and Khrievono Kikhi for technical assistance, Michelle Collins, Zacharias Kontarakis and Albert Wang for comments on the manuscript, and members of the Stainier lab for sharing reagents and discussions. This work was supported by the HumEn project funded by the European Commission's Seventh Framework Programme for Research (agreement 602587) as well as funding from the Max Planck Society to D.Y.R.S. P.D.S.D. and J.J.L. are funded by the W. M. Keck Foundation (2017-01) and NIH (U01DK105541). No potential conflicts of interest relevant to this article were reported.

C.S.M.H. and D.Y.R.S. conceived the project. C.S.M.H., S.T.M., L.M.M., F.S.M. and D.Y.R.S. contributed to discussion of data and manuscript preparation. R.B., M.L., S.O., O.K. reviewed/edited the manuscript. C.S.M.H., S.T.M., L.M.M., F.S.M., F.K., J.P., S.T., O.S., H.K., P.D.S.D. and J.J.L. generated data. C.S.M.H. and D.Y.R.S. are the guarantors of this work and, as such, had full access to all the data presented in the study and take responsibility for the data and the accuracy of the data analysis.

Figures

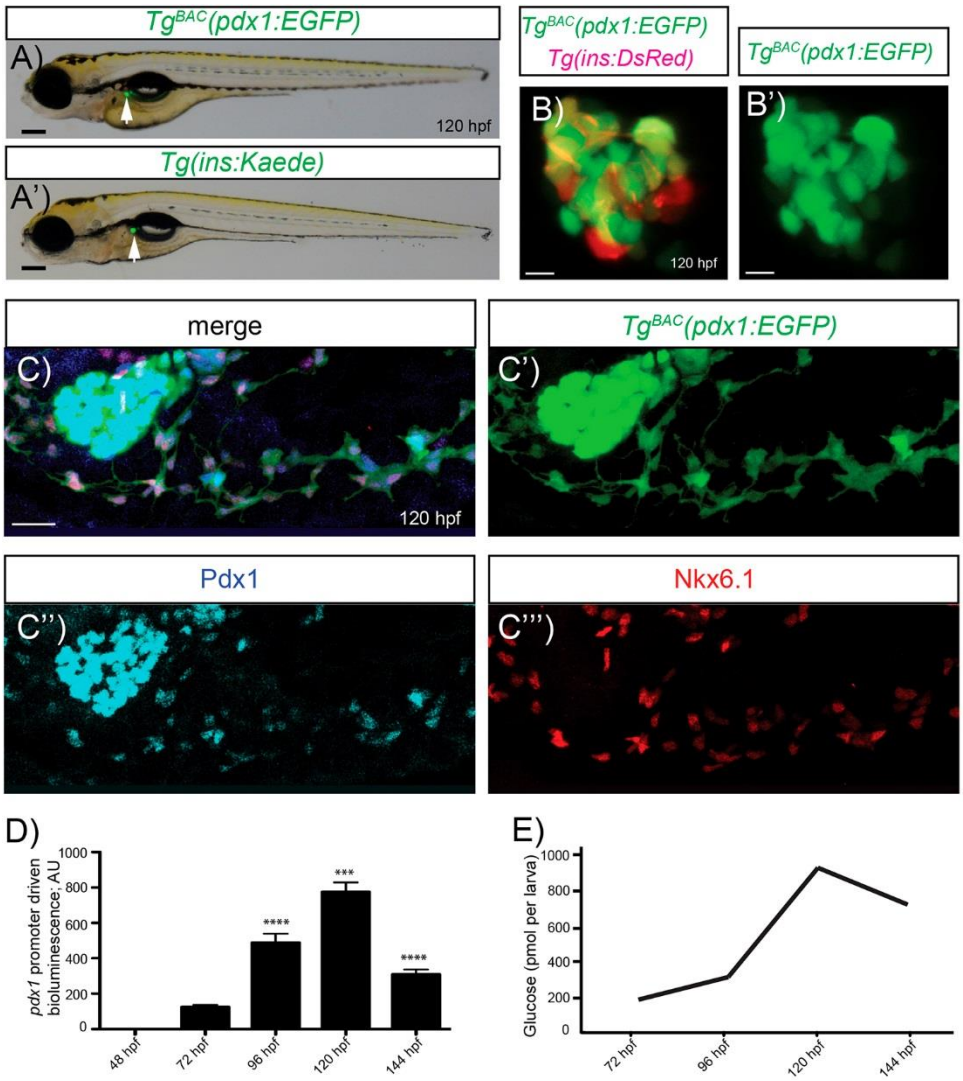

Fig.1 *pdx1* expression in β- and ductal cells

A) Visualization of *Tg*^{BAC}*(pdx1:*EGFP*)* expression. A 200 kb *pdx1* BAC drives EGFP expression specifically in the pancreatic islet (arrows). Pancreatic β-cell specific reporter signal in *Tg(ins:Kaede)* larva is shown for comparison. B) Confocal images of the pancreatic islet of a 120 hpf *Tg*^{BAC}*(pdx1:EGFP); Tg(ins:DsRed)* larva showing β-cell *Tg*^{BAC}*(pdx1:*EGFP*)* expression. C) Confocal images of the pancreas of a 120 hpf *Tg*^{BAC}*(pdx1:EGFP)* larva immunostained for GFP, Pdx1 and Nkx6.1 showing colocalisation of *Tg*^{BAC}*(pdx1:*EGFP*)* expression with endogenous Pdx1. D) Dynamics of *pdx1* promoter activity over time as measured by *Tg*^{BAC}(*pdx1*:luciferase) activity. The *Tg*^{BAC}(*pdx1*:luciferase) signal starts to become detectable at 72 hpf, peaks at 120 hpf and decreases by144 hpf. E) At the peak of the *Tg*^{BAC}(*pdx1*:luciferase) signal, whole body free glucose levels start to decrease, indicating β-cell function. AU, arbitrary units; p-values: * for $p \leq 0.05$, ** for $p \leq 0.01$, and *** for $p \leq 0.001$. Scale bars: A, 200 µm; B, B', 8 µm; C, 20 µm.

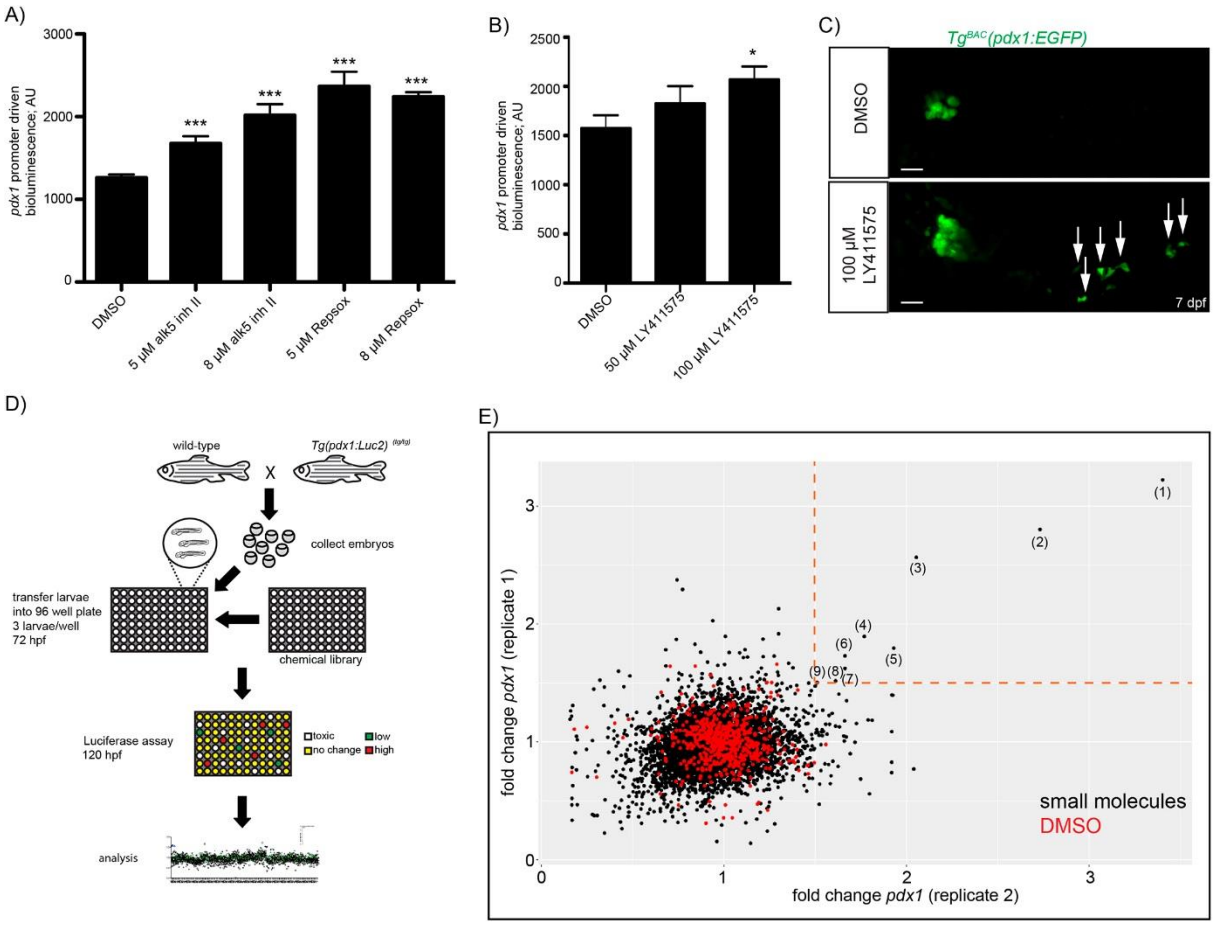

Fig. 2 Whole organism screen for modulators of *pdx1* expression

A) 48 hour treatment of 72 hpf *Tg^BAC(pdx1:Luc2)* larvae with two TGF-β inhibitors which increase *pdx1* mRNA levels in human islets leads to an increase in Luciferase activity. B) 48 hour treatment of 72 hpf *Tg^BAC(pdx1:Luc2)* larvae with the γ-secretase inhibitor LY411575, which leads to increased differentiation of β-cells, leads to an increases in Luciferase activity. C) 96 hour treatment of 72 hpf *Tg^BAC(pdx1:EGFP)* larvae with LY411575 leads to secondary islet formation as marked by *Tg^BAC(pdx1:*EGFP*)* expression (arrows). D) Establishment of high throughput screening pipeline. Mating wild-type zebrafish with homozygous *Tg^BAC(pdx1:Luc2)* reporter zebrafish generates clutches of 100% hemiozygous embryos. At 72 hpf, 3 larvae were transferred to each well of a 96 well plate and incubated for 48 hours with a specific compound at 10 μM. At 120 hpf, each plate was incubated with long half-life luciferin and the bioluminescence intensity of each well measured in a standard plate reader. E) Results of the primary screen. Differential *pdx1* promoter driven luciferase activity by small molecules of both duplicates is shown. A total of 8,256 compounds from nine bioactive small molecule libraries were screened in duplicate. Each axis represents the levels of *pdx1* reporter expression fold change from one of the duplicates. Dashed orange lines indicate 1.5-fold change. Red dots, negative control (1% DMSO); black dots, small molecules. (1) XL147; (2) SKF-86055; (3) Chaulmoogric ethyl ester; (4) VPA; (5) HC Toxin; (6) SB-736290; (7) PD168493; (8) Scriptaid; (9) 2',3'-O-Isopropylideneadenosine. p-values: * for $p \leq 0.05$, ** for $p \leq 0.01$, and *** for $p \leq 0.001$. Scale bar: C, 20 μm.

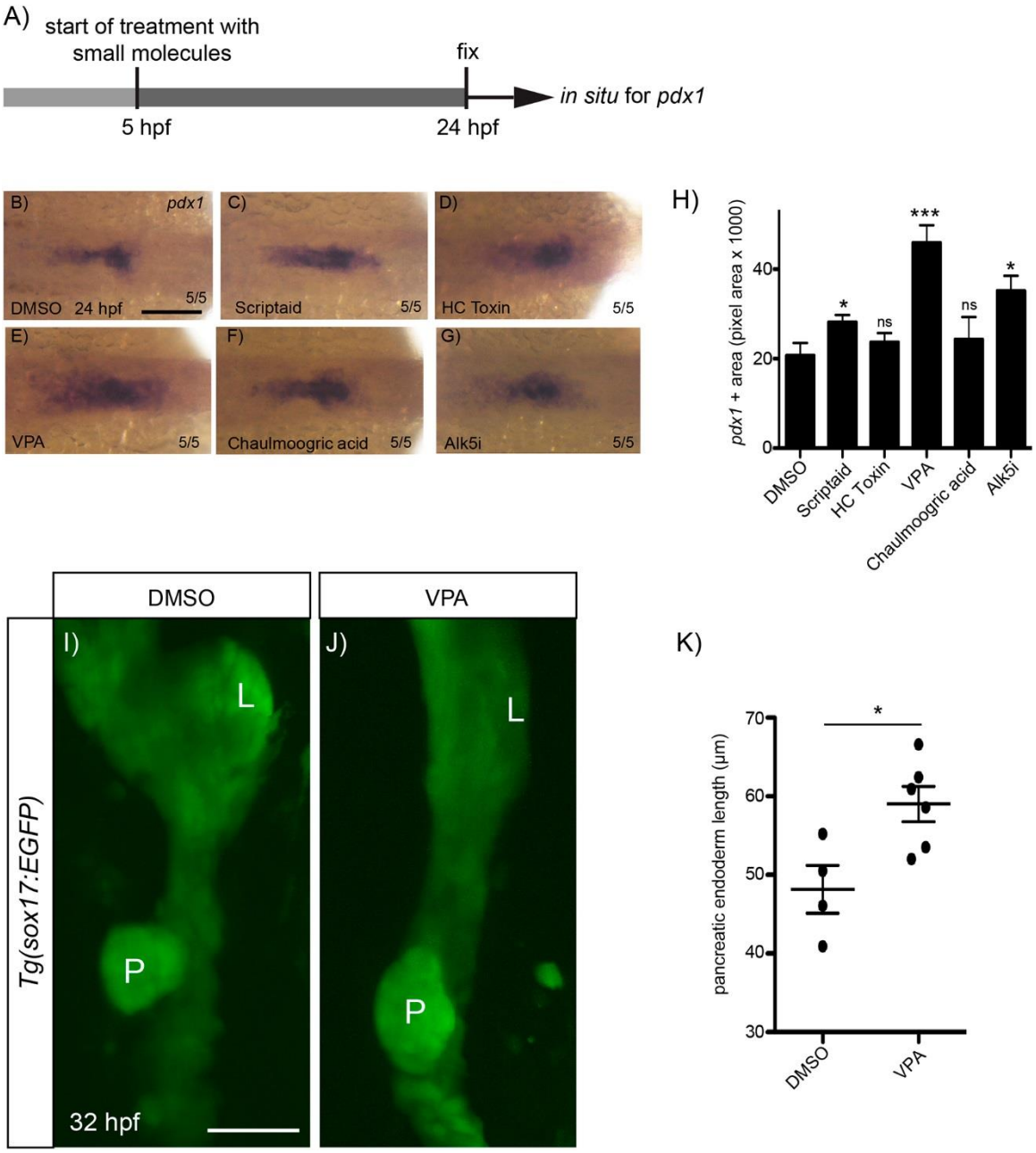

Fig. 3 HDAC inhibitor VPA increases pancreatic endoderm at the expense of hepatic endoderm

A) Schematic of the experimental set up. B-G) *in situ* hybridization on 24 hpf embryos showing *pdx1* expression. H) Scriptaid, VPA and Alk5i treatment lead to an increase in the *pdx1* positive area. I-K) Confocal pictures of 32 hpf *Tg(sox17:EGFP)* embryos treated with DMSO (I) as control or VPA (J). K) VPA treatment leads to an increase in pancreatic endoderm area. p-values: * for $p \leq 0.05$, ** for $p \leq 0.01$, and *** for $p \leq 0.001$. Scale bars: B, 100 µm; H, 20 µm.

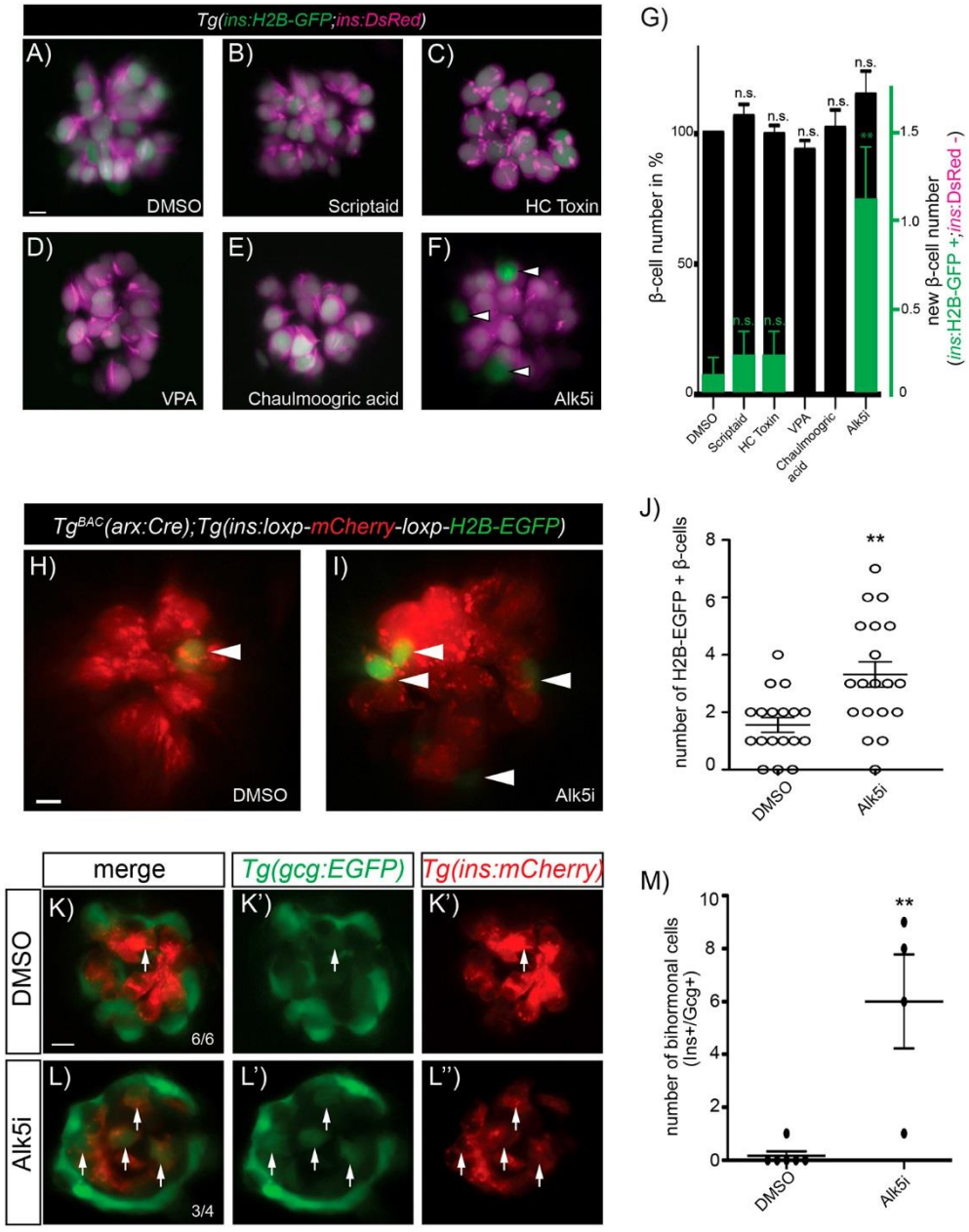

Fig. 4 Alk5 inhibition increases β-cell mass by transdifferentiation of α-cells to β-cells
Confocal pictures of 120 hpf *Tg(ins:H2B-GFP;ins:DsRed)* larvae used to count β-cells. *Tg(ins:H2B-GFP;ins:dsRED)* larvae treated with DMSO (A), Scriptaid (B), HC Toxin (C), VPA (D), Chaulmoogric acid (E), or Alk5i (F) from 72-120 hpf. Newly differentiated β-cells, labelled by H2B-GFP expression but negative for DsRed expression, are marked by arrowheads. G) None of the treatments leads to a significant increase in total β-cell numbers. Alk5 inhibition leads to an increase of newly differentiated β-cells. H-I) Confocal pictures of 120 hpf *Tg^{BAC}(arx:Cre)*; *Tg(insulin:loxP:mCherrySTOP:loxP:H2B-GFP)* larvae used to count α-cell derived β-cells (arrowheads). J) Alk5 inhibition leads to an increased number of H2B-EGFP positive β-cells. K-L) Confocal pictures of 120 hpf *Tg(gcg:EGFP)*; *Tg(insulin:mCherry)* larvae used to count bihormonal endocrine cells (arrowheads). M) Alk5 inhibition leads to an increased number of bihormonal endocrine cells. p-values: * for $p \leq 0.05$, ** for $p \leq 0.01$, and *** for $p \leq 0.001$. Scale bars: A, H, 5 µm; K, 7 µm.

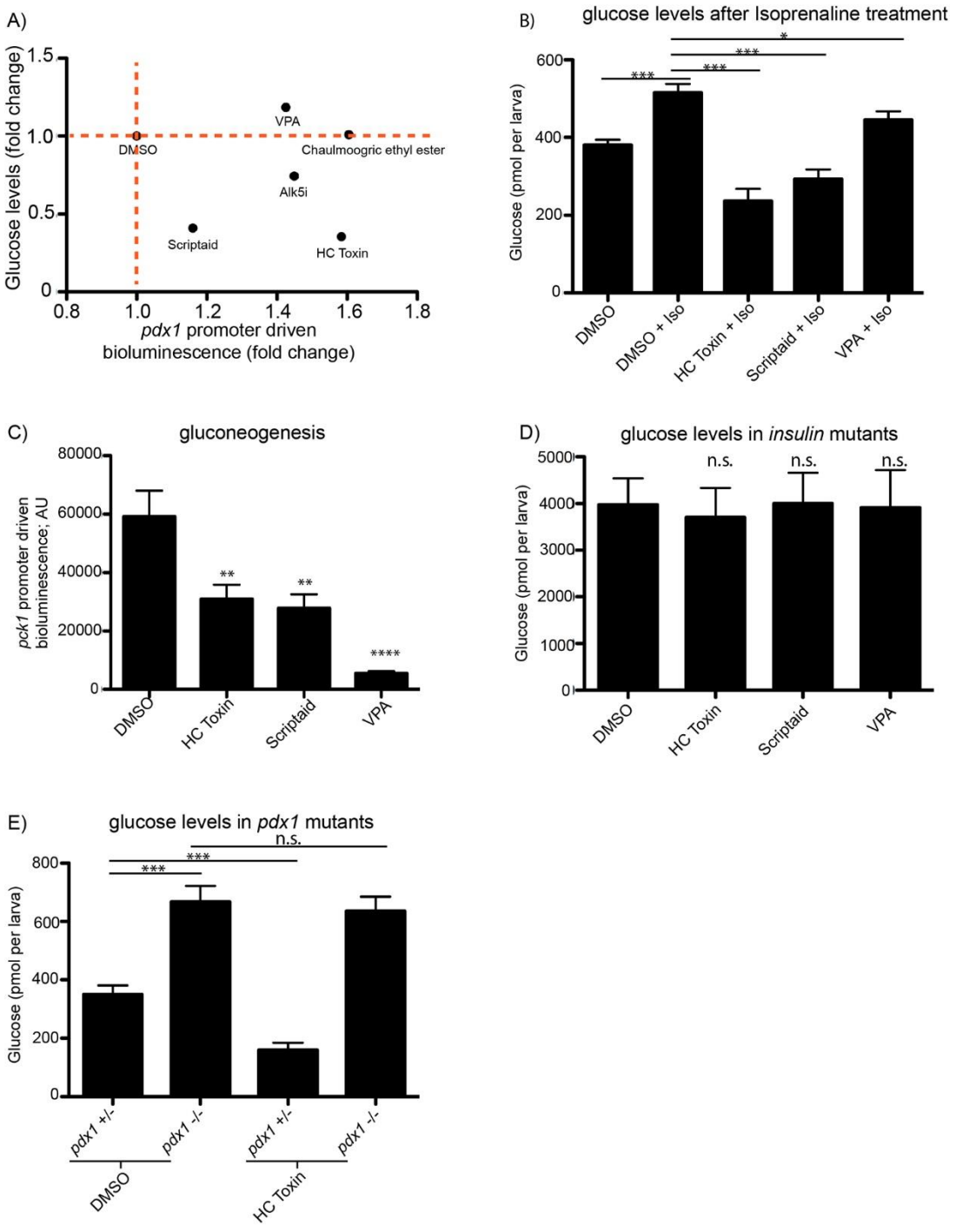

Fig. 5 Upregulation of *pdx1* expression positively regulates β-cell function

A) Scatter plot of the hits of the primary screen comparing activation of the *Tg*^{BAC}*(pdx1:Luc2)* reporter to glucose levels. B) Glucose levels after treatment with hit compounds under hyperglycaemic conditions (isoprenaline-stimulated gluconeogenesis). C) Treatment of the *Tg(pck1:Luc2)* line from 72-120 hpf with the three HDAC inhibitors leads to a reduction in Luciferase activity. D) Glucose levels in *insulin* mutants treated with the three HDAC inhibitors. E) Glucose levels in *pdx1* heterozygous and homozygous mutant animals. p-values: * for $p \leq 0.05$, ** for $p \leq 0.01$, and *** for $p \leq 0.001$.

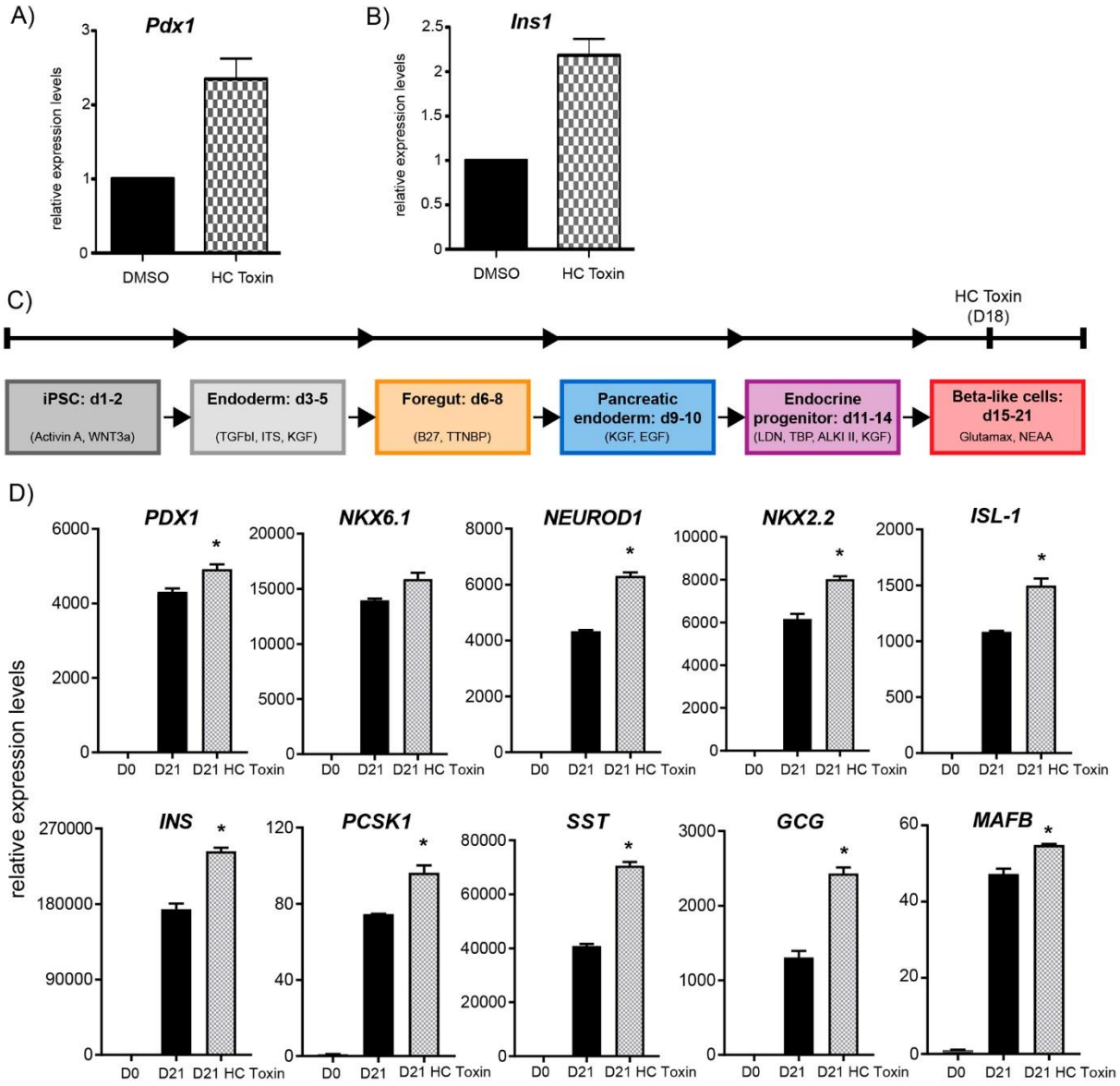

Fig. 6 HC Toxin induces the expression of β-cell differentiation markers *in vitro*

A) qRT-PCR of *Pdx1* mRNA expression levels in MIN6 cells treated with HC Toxin for 24 h. HC Toxin induces *Pdx1* expression. B) qRT-PCR of *Insulin1* (*Ins1*) mRNA expression levels in MIN6 cells treated with HC Toxin for 24 h. HC Toxin induces *Ins1* expression. C) Schematic representation of the differentiation protocol of iPSCs into β-like cells. Cells were treated with HC Toxin for 24 h at day (D)18 of differentiation. D) RT-qPCR analysis of selected gene expression levels at D0 (undifferentiated iPSCs), D21 (differentiated cells) and D21 HC (differentiated cells following treatment with HC Toxin), values are average ± SE; *, p-values: $p \leq 0.05$.

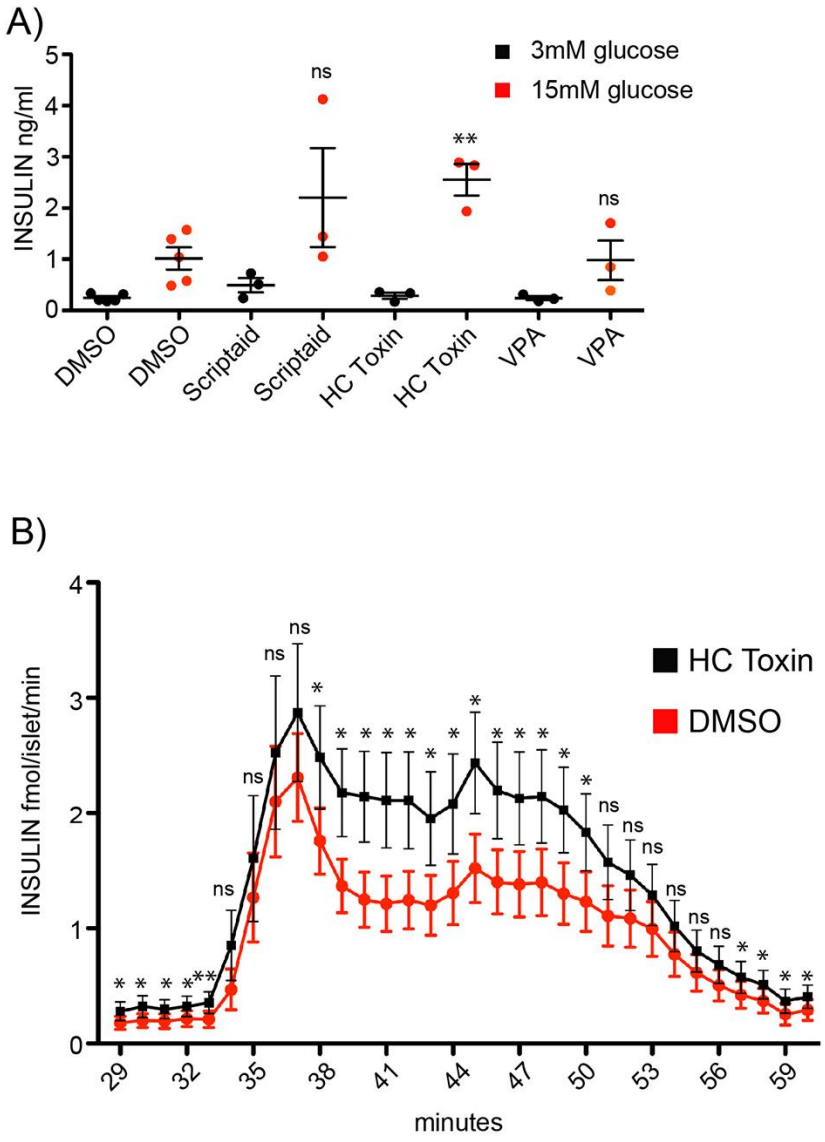

Fig. 7 HC Toxin positively regulates β-cell function in primary mouse and human β-cells
A) Insulin levels from wild-type mouse islets treated with DMSO, Scriptaid, HC Toxin, VPA for 16 h in a static GSIS assay. HC Toxin increases GSIS. B) Insulin levels from human donor islets incubated for 24 h with DMSO and HC Toxin in a perfusion assay. HC Toxin increases GSIS (n=islets of 12 human donors). p-values: * for $p \leq 0.05$, ** for $p \leq 0.01$, and *** for $p \leq 0.001$.

Figure S1

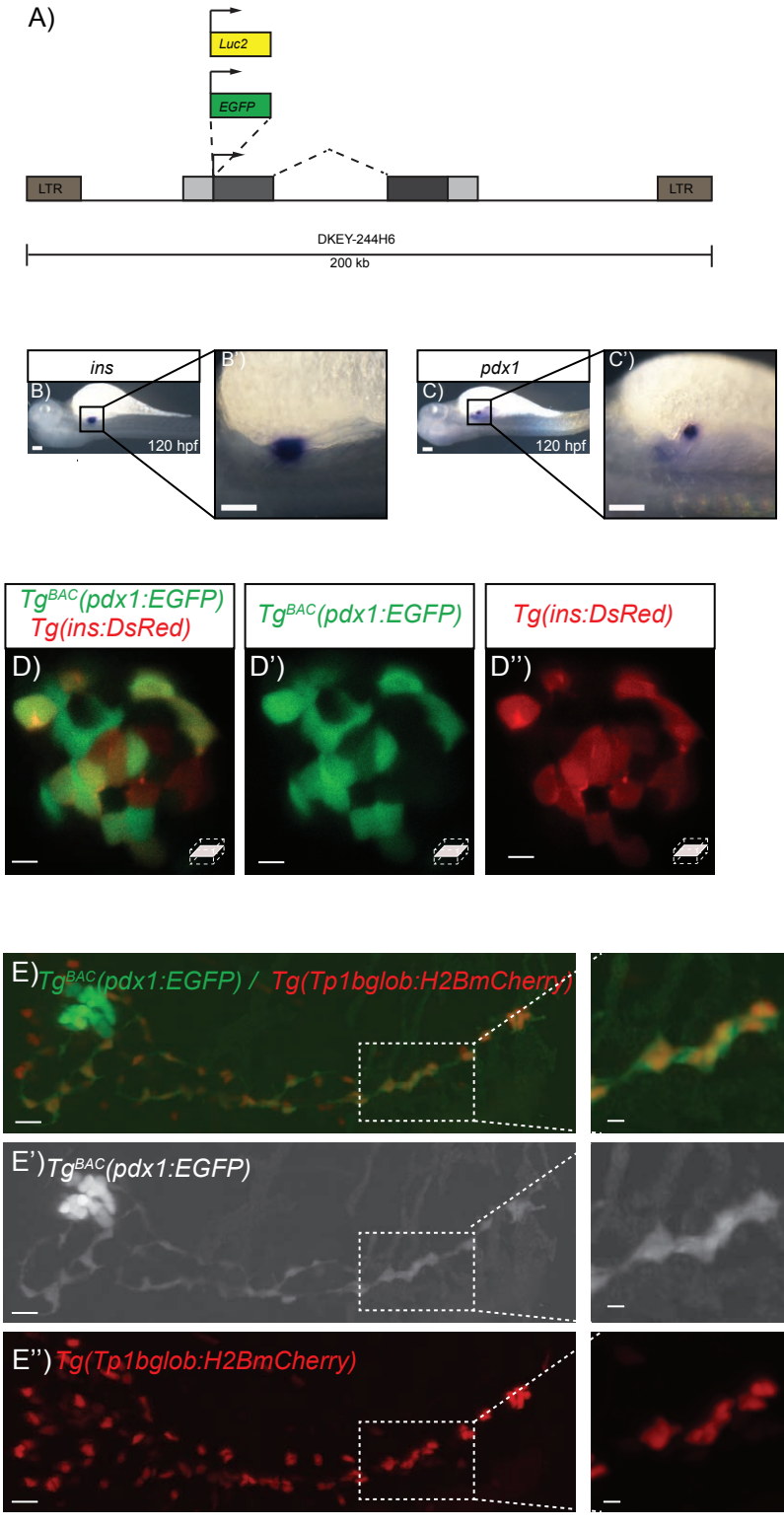

Fig. S1 Generation and validation of the *Tg^{BAC}(pdx1:EGFP)* reporter line
A) BAC engineering used to generate *Tg^{BAC}(pdx1:EGFP)* and *Tg^{BAC}(pdx1:Luc2)*. The 200 kb BAC DKEY-244H6 was engineered to carry an EGFP or Luciferase downstream of the *pdx1* ATG. To enhance the frequency of insertion into the genome, we added *tol2* arms on the backbone of the BAC. B) *in situ* hybridization on 120 hpf zebrafish larvae for *insulin* (*ins*) expression. C) *in situ* hybridization on 120 hpf zebrafish larvae for *pdx1 expression*. D) Single confocal planes of the pancreatic islet of a 120 hpf *Tg^{BAC}(pdx1:EGFP); Tg(ins:DsRed)* larva showing β-cell specific *Tg^{BAC}(pdx1:*EGFP*)* expression. E) Confocal images of the pancreas of a 120 hpf *Tg^{BAC}(pdx1:EGFP); Tg(Tp1bglob:H2BmCherry)* larva showing *Tg^{BAC}(pdx1:*EGFP*)* expression in the pancreatic duct. Scale bars: B, 100 µm; C, 100 µm; D, 5 µm; E, 15 µm.

Figure S2

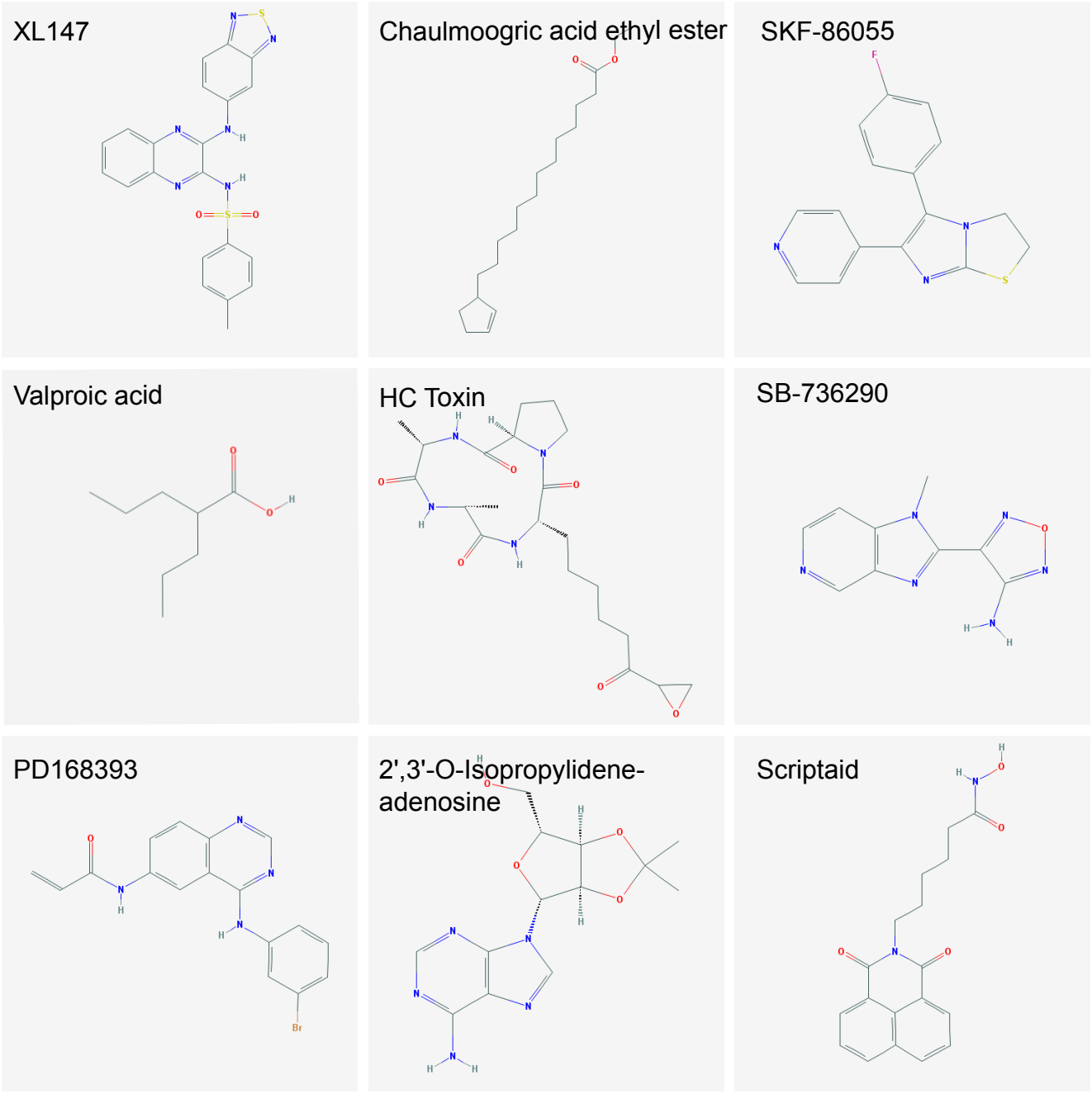

Fig. S2 Structure of the hit molecules identified in the primary screen

Figure S3

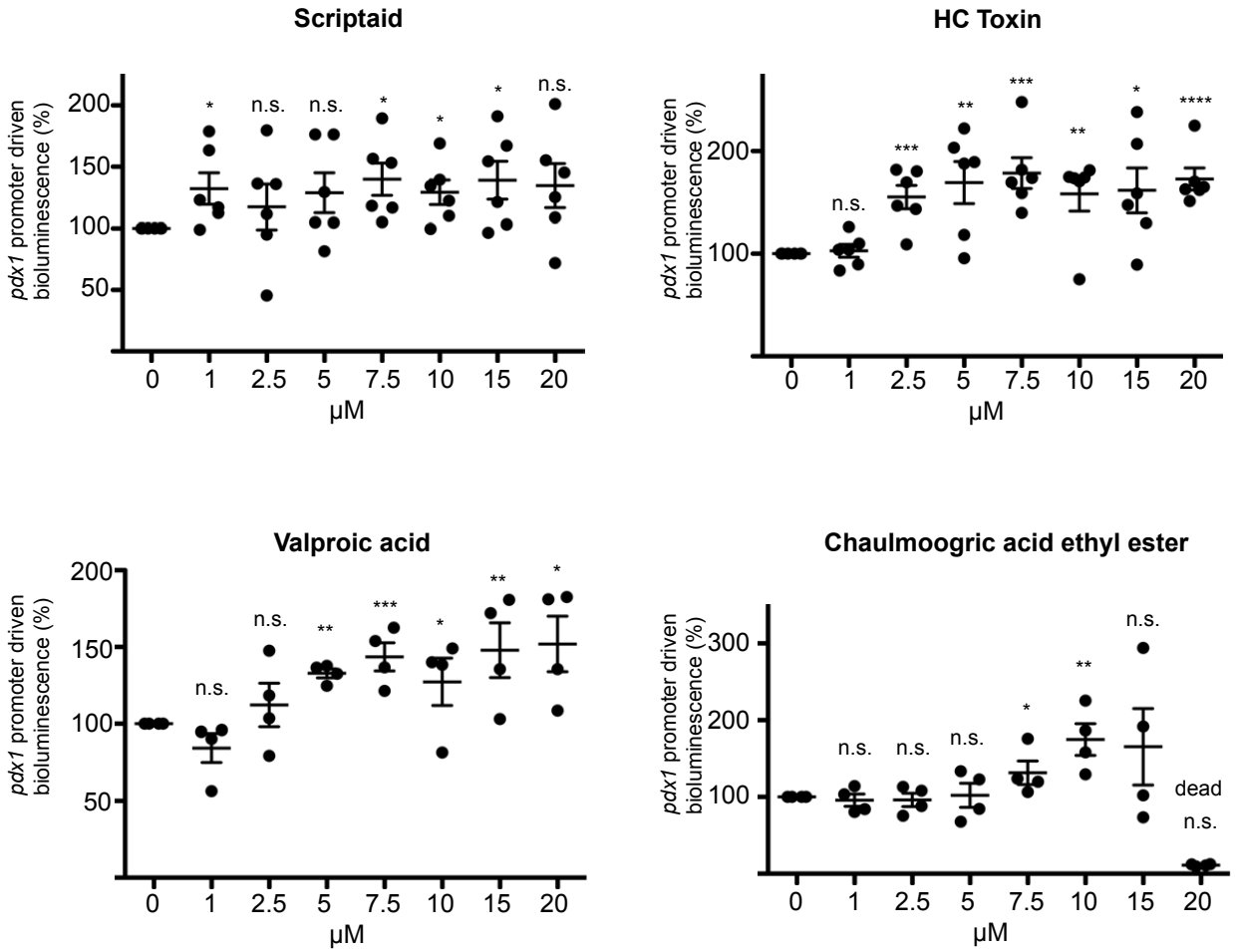

Fig. S3 Dose response curves

Dose response curves with freshly ordered Scriptaid, HC Toxin, VPA and Chaulmoogric ethyl ester show activation of the *Tg*^{BAC}*(pdx1:Luc2)* reporter. Treatment of Chaulmoogric acid ethyl ester at 20 μM leads to the death of the larvae. p-values: * for p≤0.05, ** for p≤0.01, and *** for p≤0.001.

Figure S4

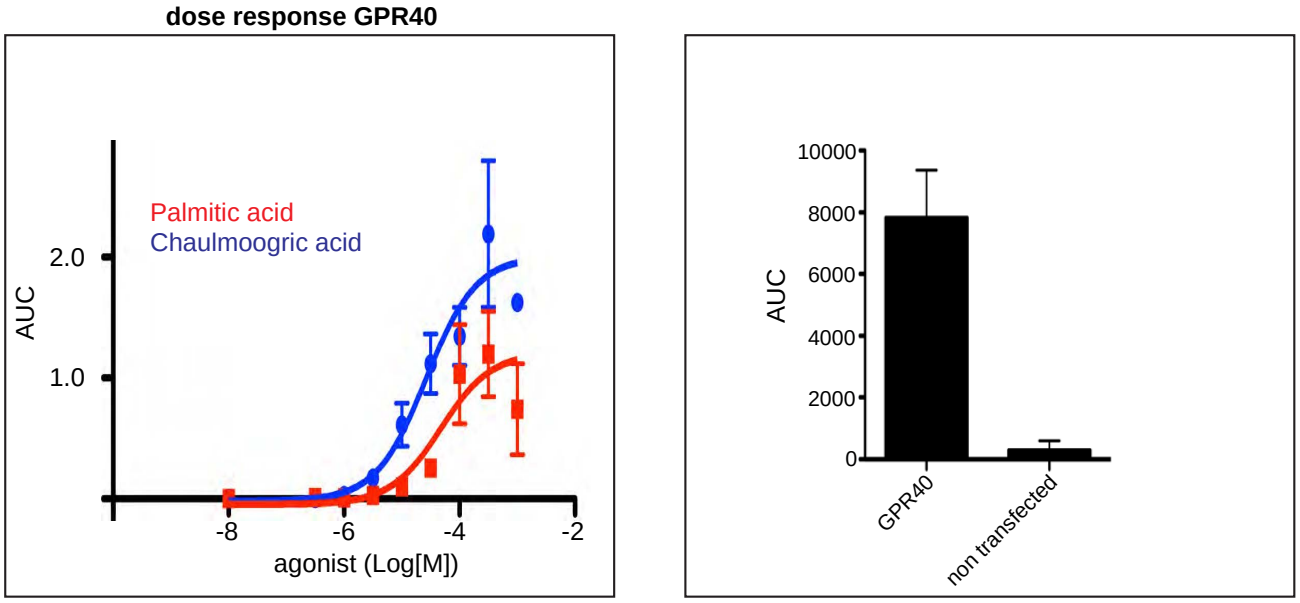

Fig. S4 Pharmacology of Chaulmoogric acid

Measurement of GPR40 activation in cells heterologously expressing human GPR40 and an intracellular calcium sensitive probe (see methods) after addition of palmitic acid or Chaulmoogric acid. Chaulmoogric acid activates GPR40. Dose response curve of Chaulmoogric acid compared to palmitic acid. No calcium traces are detected in non-transfected cells. AUC, area under the curve.

Figure S5

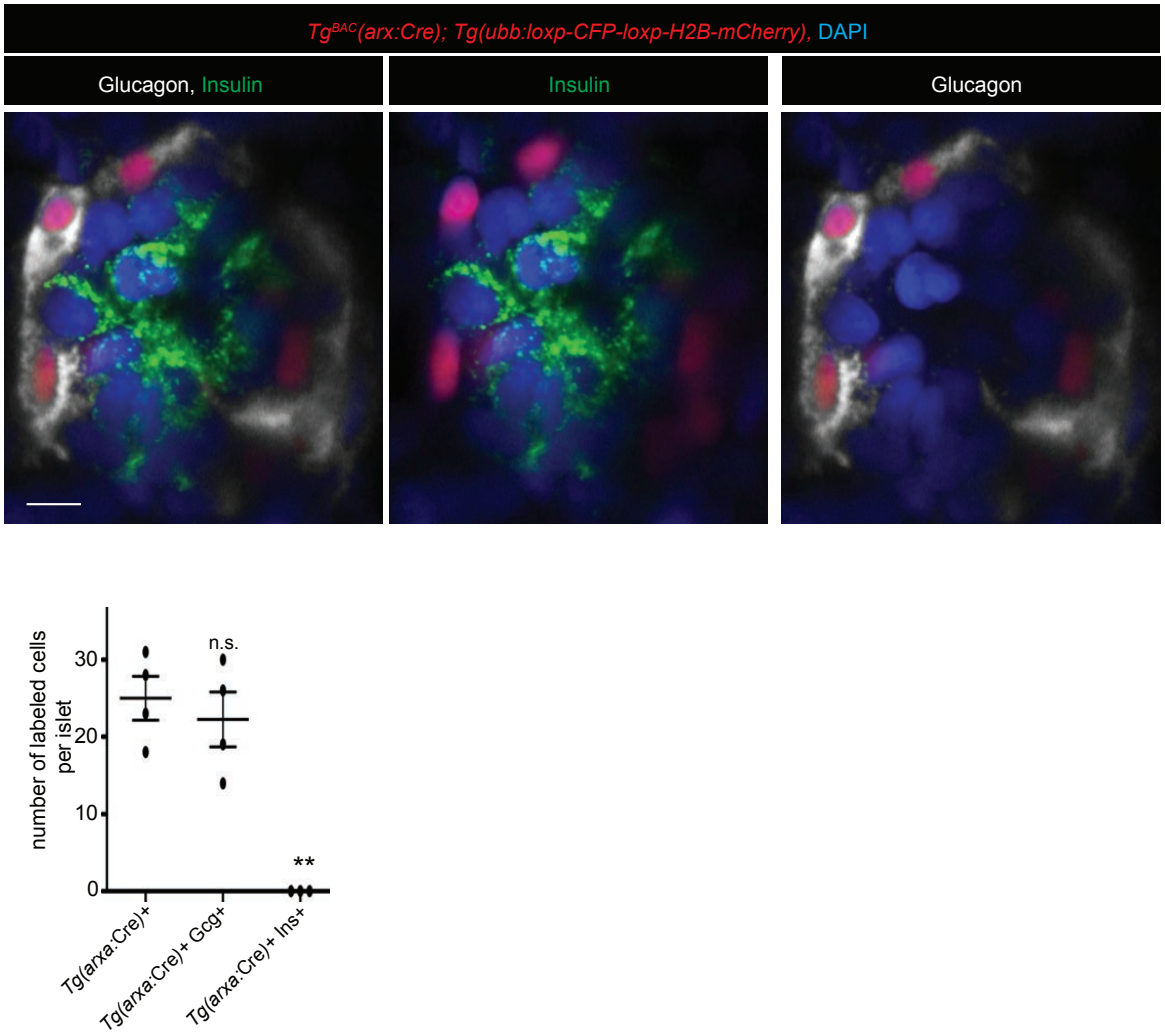

Fig. S5 Validation of the *Tg^BAC(arx:Cre)* reporter line

Confocal picture of a 120 hpf *Tg^BAC(arx:Cre)*; *Tg(ubb:loxP:CFP:loxP:H2B-GFP)* larva immunostained for Glucagon and Insulin showing Cre recombination in α-cells. Glucagon expressing α-cells are labeled by the *Tg^BAC(arx:Cre)* while Insulin expressing β-cells are not labelled. p-values: * for $p \leq 0.05$, ** for $p \leq 0.01$, and *** for $p \leq 0.001$. Scale bar: 3 µm

Figure S6

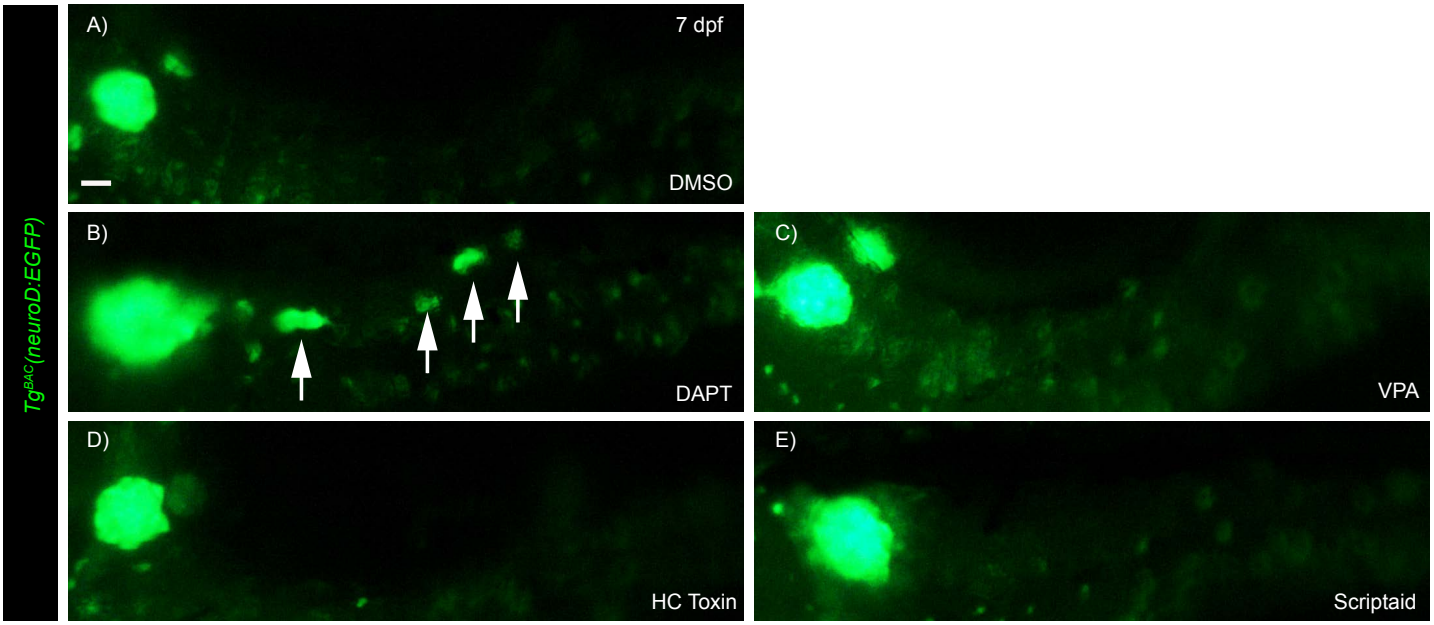

Fig. S6 Hit molecules do not induce secondary islet formation

Animals from the pan-endocrine reporter line *Tg*^{BAC}*(neuroD:EGFP)* were treated with the different HDAC inhibitors VPA, HC Toxin and Scriptaid as well as the positive control DAPT for 96 hours starting at 72 hpf. Arrows point to secondary islets. Scale bar: 20 µm.

Figure S7

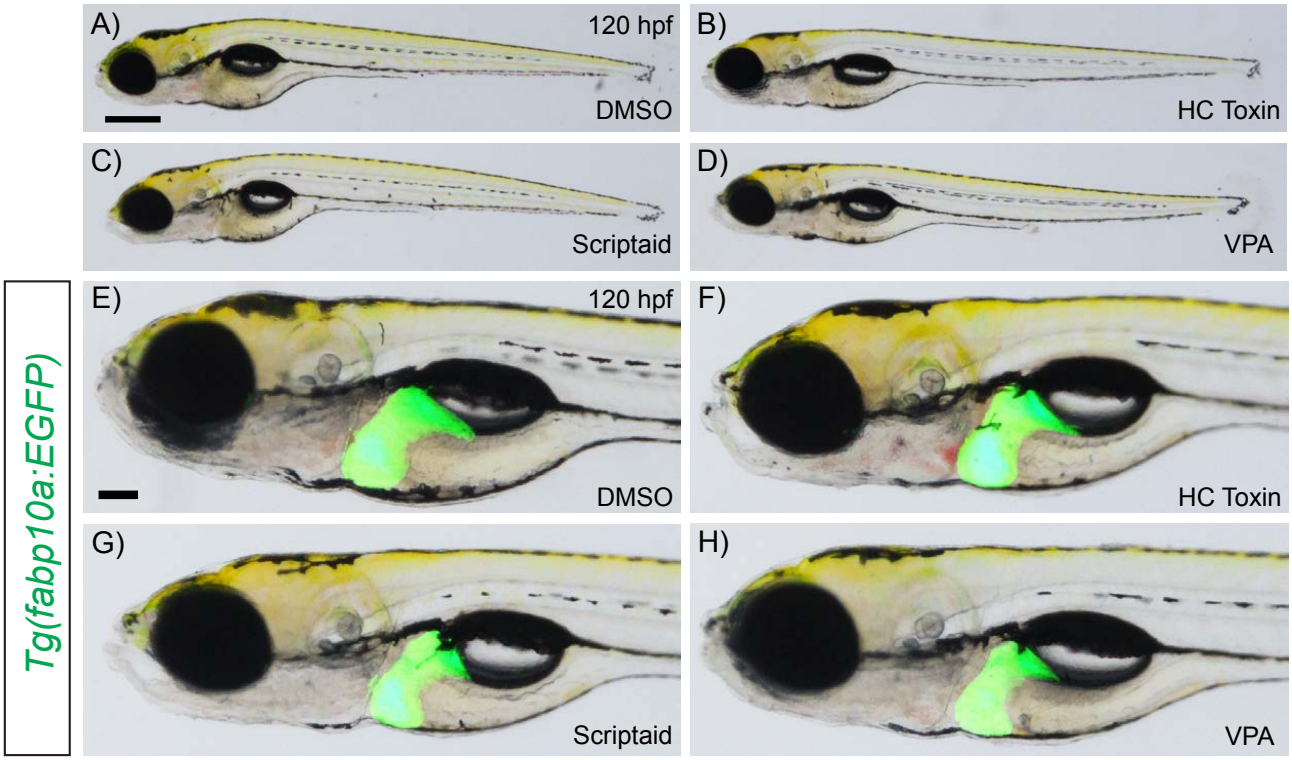

Fig. S7 Hits compounds do not show signs of toxicity

Treatment with HC Toxin, Scriptaid or VPA does not appear to affect the general health of the animals or induce liver toxicity. Animals treated for 48 hours starting at 72 hpf. Scale bars: 100 µm.

Table S1 Drugs identified to modulate *pdx1* expression in zebrafish larvae. Replicate 1 and replicate 2 represent the levels of *pdx1* reporter expression fold change.

replicate 1	replicate 2	name	function	library
3,4	3,22	S1118; XL147	PI3K inhibitor	Kinase library; Selleckchem
2,05	2,56	CHAULMOOGRIC ACID, ETHYL ESTER	fatty acid, GPR40 agonist	Spectrum Collection, Microsource
2,73	2,8	SKF-86055	Alk5 inhibitor	PKIS
1,93	1,79	Valproic acid	HDAC inhibitor	Epigenetic Screening Library, Cayman
1,76	1,89	HC Toxin	HDAC inhibitor	Epigenetic Screening Library, Cayman
1,66	1,73	SB-736290	MSK1 inhibitor	PKIS
1,61	1,51	S7039; PD168393	EGFR inhibitor	Kinase library; Selleckchem
1,51	1,5	2',3'-O-Isopropylideneadenosine	adenosine receptor agonist	Natural Compounds; TimTech
1,51	1,5	Scriptaid	HDAC inhibitor	Epigenetic Screening Library, Cayman

Table S2 Characteristics of human pancreatic islet donors.

Donor #	Age	Sex	BMI (kg/m2)	HbA1c
1	64	F	23	5,8
2	61	M	37	6,1
3	34	M	26,3	5,3
4	66	F	25,7	5,7
5	72	F	22,7	5,5
6	77	M	27,4	5,6
7	56	F	24,2	5,7
8	70	M	23,4	5,8
9	62	M	24,7	5,4
10	55	F	27	5,5
11	67	F	23,7	5,6
12	65	M	23,1	5,6

Table S3 Primers for RT-qPCR

Gene	Primer name	Sequence (5' to 3')
NEUROD1	NEUROD1-F	GACACGAGGAATTCGCCCAC
	NEUROD1-R	CCCACTCTCGCTGTACGATTT
NKX6.1	NKX6.1-F	TGGCCTATTCGTTGGGGATG
	NKX6.1-R	TGTCTCCGAGTCCTGCTTCT
ISL1	ISL1-F	ACATGCTTTGTTAGGGATGGGA
	ISL1-R	TCGTTCTTGCTGAAGCCGAT
GAPDH	GAPDH-F	AGCTCACTGGCATGGCCTTC
	GAPDH-R	CGCCTGCTTCACCACCTTCT
SST	SST-F	CCACTCTCCAGCTCGGCTTT
	SST-R	TTGGCCAGTTCCTGCTTCCC
PDX1	PDX1-F	CACATCCCTGCCCTCCTAC
	PDX1-R	GAAGAGCCGGCTTCTCTAAAC
MAFB	MAFB-F	CCCGACCGAACAGAAGACA
	MAFB-R	ACTGGGTGCGAGCCGATGAG
PCSK1	PCSK1-F	GCTAAATGCCAAAGCTCTGGTGG
	PCSK1-R	GCTTTCAGGGCTCTGGGCTC
GCG	GCG-F	GCAACGTTCCCTTCAAGACAC
	GCG-R	ACTGGTGAATGTGCCCTGTG
INS	INS-F	CAGAAGAGGCCATCAAGCAG
	INS-R	CTTGGGTGTGTAGAAGAAGCC
NKX2.2	NKX2.2-F	TTCCAGAACCACCGCTACAAG
	NKX2.2-R	GGGCGTCACCTCCATACCT

Table S4 Ct values for RT-qPCR

cells	gene	Average Ct value HC Toxin	Average Ct value DMSO	Ct Value housekeeping gene HC Toxin	Ct Value housekeeping gene DMSO
MIN6	*Pdx1*	21,86	22,36	21,16	20,37
MIN6	*Ins1*	15,61	16,00	21,16	20,37
iPSC	*PDX1*	21,91	22,09	19,88	19,86
iPSC	*NKX6.1*	21,70	21,87	19,88	19,86
iPSC	*NEUROD1*	22,45	22,98	19,88	19,86
iPSC	*INS*	18,47	18,84	21,59	21,48
iPSC	*SST*	18,74	19,42	21,59	21,48
iPSC	*NKX2.2*	23,11	23,41	20,69	20,62
iPSC	*ISL-1*	23,85	24,19	20,13	20,01
iPSC	*GCG*	18,52	19,31	20,13	20,01
iPSC	*PCSK1*	23,9	24,2	20,34	20,27
iPSC	*MAFB*	23,14	23,3	20,34	20,27